

A Change-Point Approach to Estimating the Proportion of False Null Hypotheses in Multiple Testing

Anica Kostic^{*†}

Piotr Fryzlewicz[†]

Abstract

For estimating the proportion of false null hypotheses in multiple testing, a family of estimators by Storey (2002) is widely used in the applied and statistical literature, with many methods suggested for selecting the parameter λ . Inspired by change-point concepts, our new approach to the latter problem first approximates the p -value plot with a piecewise linear function with a single change-point and then selects the p -value at the change-point location as λ . Simulations show that our method has among the smallest RMSE across various settings, and we extend it to address the estimation in cases of superuniform p -values. We provide asymptotic theory for our estimator, relying on the theory of quantile processes. Additionally, we propose an application in the change-point literature and illustrate it using high-dimensional CNV data.

Keywords: Multiple testing; change-point detection; p -values

1 Introduction

Of interest to us in this work is the problem of estimating the proportion of false null hypotheses when many are tested simultaneously. Under the standard assumption of uniformity of true null p -values, p -value distribution is modeled as a mixture, with cumulative distribution function (CDF)

$$F(x) = \pi_1 F_1(x) + \pi_0 x, \quad x \in [0, 1], \quad (1)$$

where π_1 is the unknown proportion of false null hypotheses, $\pi_0 = 1 - \pi_1$ and F_1 is the CDF of the p -values under the alternative (Storey, 2002; Meinshausen and Rice, 2006; Patra and Sen, 2016).

Estimating the false null proportion π_1 comes down to the problem of estimating the proportion parameter of the mixture distribution, particularly when one component is known. This measure quantifies the overall magnitude of significant deviations from baseline non-significant behavior, making it independently valuable. Furthermore, this measure is of interest in the classification literature, mainly when only positive and unlabeled examples

^{*}Author for correspondence. [E-mail: a.kostic@lse.ac.uk, Address: Department of Statistics, London School of Economics and Political Science, Columbia House, Houghton Street, London, WC2A 2AE, UK]

[†]London School of Economics and Political Science

are available (Blanchard et al., 2010; Jain et al., 2016, 2017). In the multiple testing literature, proportion estimators are mainly of indirect interest as they can be used to increase the power of multiple testing procedures, such as the Benjamini-Hochberg procedure by Benjamini and Hochberg (1995) (BH), that controls the false discovery rate (FDR). Incorporating a proportion estimator into the BH procedure is originally proposed in Benjamini and Hochberg (2000), where the authors suggest increasing the number of rejections by increasing the threshold while keeping the FDR controlled at a desired level approximately. The proportion parameter is also valuable in practical applications, particularly in astronomy and astrophysics (Meinshausen and Rice, 2006; Patra and Sen, 2016; Swanepoel, 1999).

Storey’s method (Storey, 2002), initially introduced in Schweder and Spjøtvoll (1982), is the most common approach to the problem of estimating the proportion parameter. Assuming that $F_1(x) \approx 1$ for sufficiently large $x \in (0, 1)$, the CDF (quantile function) of the p -values is approximately linear with slope π_0 ($1/\pi_0$). Storey’s family of plug-in true null proportion estimators is

$$\hat{\pi}_0(\lambda) = \frac{1 - \hat{F}_n(\lambda)}{1 - \lambda}, \quad \lambda \in (0, 1), \quad (2)$$

and $\hat{\pi}_1(\lambda) = 1 - \hat{\pi}_0(\lambda)$. There are multiple estimators in the literature based on Storey’s family, each proposing different tuning parameter values, with no general agreement on the optimal value of λ (Benjamini and Hochberg, 2000; Storey and Tibshirani, 2003; Storey et al., 2004; Jiang and Doerge, 2008). In general, a smaller λ introduces higher bias, while choosing λ close to 1 increases the variance of the proportion estimator. Asymptotically, Storey’s estimator is guaranteed not to overestimate π_1 for any λ . The properties of consistency and asymptotic normality of this estimator are examined in Genovese and Wasserman (2004).

In this paper, we propose a new data-driven method for tuning Storey’s estimator, which we call “Difference of Slopes” or DOS. We propose to approximate the plot of sorted p -values $(i, p_{(i)})$, $i = 1, \dots, n$, with a piecewise linear function with a single change in slope, using a statistic inspired by the change-point literature. If $1 \leq \hat{k} \leq n$ is the estimated change-point location, we set $\lambda = p_{(\hat{k})}$ in Storey’s estimator (2) to obtain the proportion estimator, referred to as “DOS-Storey”. This value of λ aims to separate true from false null p -values. Specifically, we aim for it to be the smallest value at which $F_1(\lambda) \approx 1$, marking the onset of the linear part in the quantile function. By choosing such λ our goal is to reduce the variance while maintaining low bias in the corresponding Storey’s estimator. An illustration of the piecewise linear approximation produced by our method is shown in Figure 1.

In the applied literature, adaptive FDR control is primarily achieved using Storey-based proportion estimators proposed in Benjamini and Hochberg (2000) (Xu et al., 2017; Taquet et al., 2021; Wittenbecher et al., 2022) and Storey and Tibshirani (2003) (Cuomo et al., 2020; Klunk et al., 2022; Legut et al., 2022; Gigante et al., 2022). However, it is noted that Benjamini and Hochberg (2000) produces very conservative estimators, while Storey and Tibshirani (2003) produces highly variable estimators (Broberg, 2005; Langaas et al., 2005; Jiang and Doerge, 2008). These two methods are among those employed in the simulation study in Section 4. The simulation results show that the proposed DOS-Storey estimator outperforms other proportion estimators under various settings, most notably when π_1 is small. Furthermore, the proposed estimator outperforms its competitors in small samples, which is particularly significant when some of the other estimators are inapplicable.

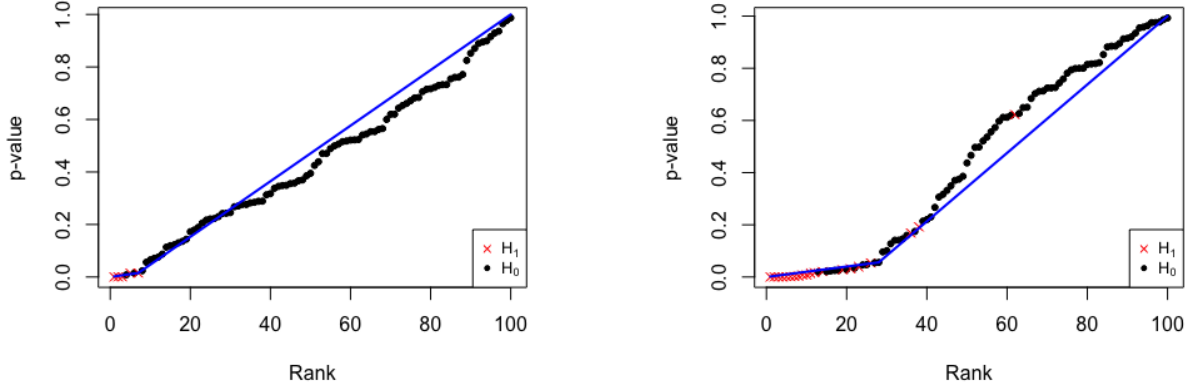


Figure 1: Illustration of our method’s piecewise linear approximation (solid line) applied to p -value plots in two settings. p -values come from Gaussian mean testing, $H_0 : \mu = 0$ versus $H_1 : \mu > 0$. The test statistics T_i have $N(0, 1)$ distribution under the null and $N(\mu_1, 1)$ under the alternative. p -values are calculated as $p_i = 1 - \Phi(T_i)$. Left (sparse case): 5 false null (crosses) and 95 true null (points) p -values, where $\mu_1 = 3$. Right (dense case): 20 false null (crosses) and 80 true null (points), where $\mu_1 = 2$.

We investigate the asymptotic properties of the DOS-Storey estimator under model (1), using results from the theory of quantile processes. The properties of the estimator depend on the unknown quantile function. However, we only impose weak assumptions on this function.

We extend our contribution by considering the case of superuniform (stochastically larger than uniform) true null p -value distributions. This scenario arises when the null hypothesis is misspecified or composite. In such cases, the linearity assumption used by Storey’s estimator does not hold, making it unsuitable to use. As an alternative, we propose to estimate the change-point in the p -value plot and to use it directly as a proportion estimator. Specifically, we define \hat{k}/n as the estimated false null proportion in this method, which we refer to as “uncorrected DOS” or uDOS. A precise definition of uDOS follows in Section 4.2. Simulations show that the uDOS estimator has a uniformly smaller mean squared error than the competing method.

Finally, in our real data example, we propose applying the DOS-Storey method in the change-point literature, illustrating it with high-dimensional copy number variation (CNV) data from neuroblastoma patients.

This paper is organized as follows. Section 2 describes our proposed method. Theoretical results are presented in Section 3, while Section 4 contains simulation results under the standard model (1), as well as in the superuniform case. The real data example can be found in Section 5. Finally, Section 6 covers the discussion and potential extensions. The code implementing the introduced approach, the simulation study, and the real data example is included in the R package MTCP, which is available at <https://github.com/anicaKostic/MTCP>.

2 DOS Threshold and the DOS-Storey Estimator

Consider the sequence of sorted p -values, $p_{(1)}, \dots, p_{(n)}$, and their representation as points $(i, p_{(i)})$ for $i = 1, \dots, n$, forming a p -value plot. The proposed piecewise linear approximation of the p -value plot is determined by the change-point location \hat{k} . It consists of a line connecting $(0, 0)$ and $(\hat{k}, p_{\hat{k}})$, and another line connecting $(\hat{k}, p_{\hat{k}})$ and $(n+1, 1)$. To calculate the change-point estimate \hat{k} , we first define the Difference of Slopes (DOS) sequence as

$$\begin{aligned} d_\alpha(i) &= \frac{p_{(2i)} - p_{(i)}}{i^\alpha} - \frac{p_{(i)}}{i^\alpha} \\ &= \frac{p_{(2i)} - 2p_{(i)}}{i^\alpha}, \end{aligned} \quad (3)$$

for some $\alpha \in [1/2, 1]$. The DOS statistic, serving as the change-point estimate, is the index of the maximum term in the DOS sequence:

$$\hat{k}_\alpha = \operatorname{argmax}_{nc_n \leq i \leq n/2} d_\alpha(i). \quad (4)$$

The choice of the non-random sequence c_n and the value of α is discussed below. The proposed separation threshold is $p_{(\hat{k}_\alpha)}$. To obtain the proportion estimate using the DOS statistic, we plug $\lambda = p_{(\hat{k}_\alpha)}$ into Storey's estimator (2) and get the proposed DOS-Storey false null proportion estimator:

$$\hat{\pi}_1^\alpha = \frac{\hat{k}_\alpha/n - p_{(\hat{k}_\alpha)}}{1 - p_{(\hat{k}_\alpha)}}. \quad (5)$$

To ensure the asymptotic results stated in Section 3 hold, we exclude the first nc_n values from $d_\alpha(i)$ from the search for maximum in (4). Precisely, the sufficient conditions are

$$\begin{aligned} \frac{nc_n}{\log \log n} &\rightarrow \infty, \\ \frac{\log \log(1/c_n)}{\log \log n} &\rightarrow C < \infty. \end{aligned}$$

In Remark 1 in the Appendix, we discuss how different rates for c_n affect the asymptotic results. The practical selection of c_n is addressed in Section 4.

An illustration of the proposed method with $\alpha = 1$ for the two examples from Figure 1 is given in Figure 2. The two plots in the right column show the dependency of $\hat{\pi}_1(\lambda)$ on λ , and the substantial influence of λ due to the bias-variance trade-off, for two different values of π_1 . In the sparse case, the estimated change-point location is at $\hat{k}_1 = 7$ and the estimated number of false nulls is $\hat{n}_1 = 4$ (true number is $n_1 = 5$). In the dense case, the change-point location is at $\hat{k}_1 = 28$ with an estimated number of false nulls of $\hat{n}_1 = 24$ ($n_1 = 20$). Figure 2 also shows how the false null p -values exceeding the threshold $p_{(\hat{k}_\alpha)}$ are relatively few compared to the true null p -values. In both scenarios, it is evident how our approach effectively reduces variance and maintains low bias in the associated Storey's estimator (5). In larger samples, this effect is best seen when the proportion of false null hypotheses is small, as shown in the simulation study in Section 4.

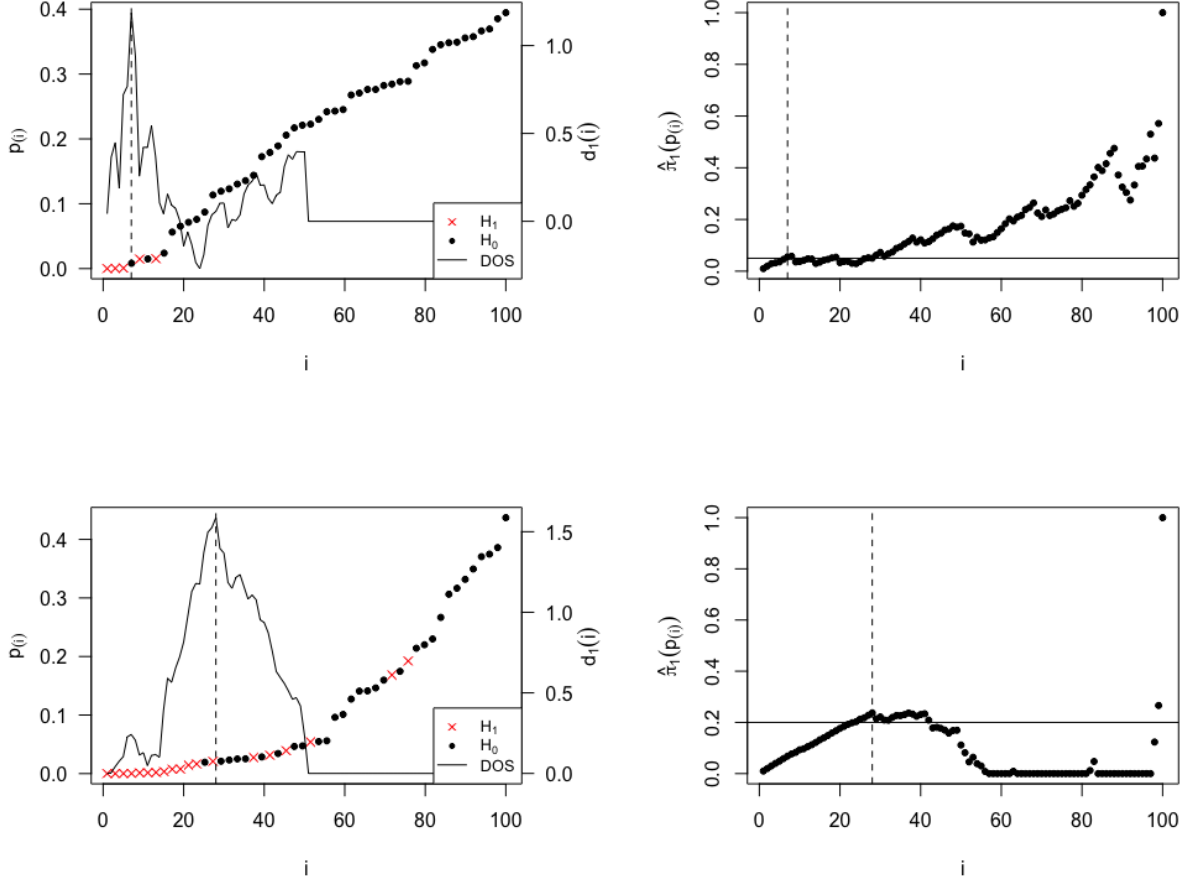


Figure 2: Illustration of the DOS method for $\alpha = 1$ for the two examples from Figure 1. Left column: p -value plot and the corresponding DOS sequence (solid line) with the estimated change-point location (vertical dashed line) in the sparse (top) and the dense (bottom) case. Right column: corresponding Storey's sequence of estimators in the sparse (top) and the dense (bottom) case; solid horizontal line is at the unknown false null proportion level, and dashed vertical line marks the proportion estimated by the DOS-Storey method.

We now provide further explanation of the DOS statistic and discuss the role of the parameter α by examining its boundary values. We begin with the case where $\alpha = 1$, and then we discuss $\alpha = 1/2$. These values enable us to interpret our statistic within the context of change-point literature.

For $\alpha = 1$, the first term in (3) is the slope of the line connecting points $(i, p_{(i)})$ and $(2i, p_{(2i)})$, while the second term corresponds to the slope of the line connecting $(0, 0)$ and $(i, p_{(i)})$. Therefore, $d_1(i)$ is the sequence of slopes differences in the p -value plot, and \hat{k}_1 is the location of the maximum slopes difference. Let $s_j = p_{(j)} - p_{(j-1)}$ be the sequence of spacings

of p -values and $p_{(0)} = 0$. The DOS sequence can be written as

$$d_1(i) = \frac{1}{i} \sum_{j=1}^i s_j - \frac{1}{i} \sum_{j=i+1}^{2i} s_j.$$

Thus, the DOS statistic finds the maximum difference of means on symmetric $((0, i), (i, 2i))$ and increasing intervals $(i = 1, \dots, n/2)$ in the spacings sequence. A similar statistic, aiming to detect shifts in the piecewise constant mean of an ordered sample, has been studied in the nonparametric change-point literature (Brodsky and Darkhovsky, 1993). Therefore, the DOS statistic can be viewed as a technique for fitting a piecewise constant function to the sequence of spacings s_i . An illustration of the piecewise constant fit to the spacings sequence is provided in Figure 3.

Similarly, for $\alpha = 1/2$, we can interpret $d_{1/2}(i)$ as the standardized difference between the means of the first i and the second i spacings. In the context of the change-point literature, the statistic $\max_i d_{1/2}(i)$ can be regarded as a CUSUM-like statistic.

In general, we use symmetric intervals $((0, i), (i, 2i))$ for calculating slopes to focus on the local behavior and changes in the quantile function. These intervals expand $(i = 1, \dots, n/2)$ to incorporate information from an increasing number of p -values until a shift to linearity is observed. As the estimated change-point is at most at location $n/2$, our method is unsuitable for cases when the proportion of false null hypotheses is high.

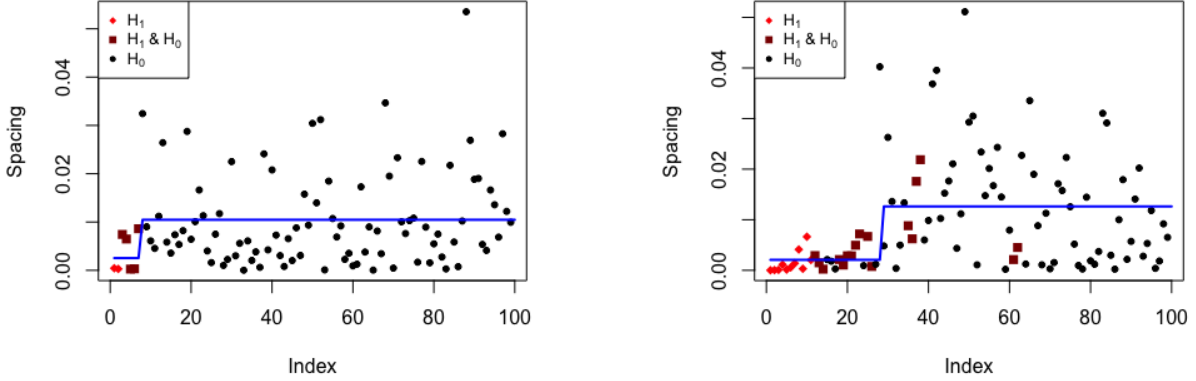


Figure 3: Illustration of the piecewise constant fit to the spacings sequence using the DOS method with $\alpha = 1$ for the two examples from Figure 1. The spacings are divided into three groups as follows: If for a given s_i , both $p_{(i)}$ and $p_{(i-1)}$ are false null, the spacing is denoted by a diamond. If both are true null, circles are used. Squares are used for cases where one p -value is true null, and the other is false null.

Using a change-point method for the purpose of tuning Storey's estimator has been previously mentioned in the literature. In Benjamini and Hochberg (2000), it is implied that a change-point method can be used for estimating the proportion of false null hypotheses by identifying the end of the linear segment in the p -value plot. This approach is explored

in Turkheimer et al. (2001) and Hwang et al. (2014). However, the simulations included in Section B.5 of the Supplementary Material show that the latter two methods do not perform well when compared to our method, and we do not include them in the simulation study.

Note that this scenario differs from the conventional change-point in the slope problem. The p -value plot has no typical change-point; instead, the change-point is linked to the suggested linear approximation. Asymptotically, the change-point location depends on the properties of the unknown quantile function and on our fitting procedure. Additionally, it is reasonable to think of our method as identifying a 'knee' in the quantile plot, a topic briefly discussed in Section C of the Supplementary Material.

3 Theoretical Considerations

We begin this section by introducing the assumptions on the p -value model introduced in (1). Following that, we present the statement of the main Theorem 1, along with two immediate corollaries. The theorem contains results regarding the asymptotic behaviour of the change-point estimator and the proportion estimator. The proof can be found in Appendix A.

Different assumptions on F_1 can be found in the literature. Strong assumptions specify a family of distributions for F_1 , see for example Cai et al. (2007) and Pounds and Morris (2003), while weaker ones only restrict its shape. We place the following two assumptions concerning F :

(A1) F_1 is a continuous distribution stochastically smaller than $U[0, 1]$, with a concave CDF.

(A2) Let

$$h_\alpha^F(t) := \frac{F^{-1}(2t) - 2F^{-1}(t)}{t^\alpha}, \quad t \in (0, 1/2). \quad (6)$$

$h_\alpha^F(t)$ has a unique point of local maximum at $\tilde{t}_\alpha \leq 1/2$.

Assumption (A1) implies that the density of the false null p -values is decreasing and is a common assumption in the literature (Langaas et al., 2005; Celisse and Robin, 2010). Assumption (A2) is specific to our approach and is necessary for uniquely defining the asymptotic change-point location. As the ordered p -values are sample quantiles, h_α^F represents the “ideal function” that the DOS sequence approximates:

$$\frac{p_{(2i)} - 2p_{(i)}}{(i/n)^\alpha} \approx h_\alpha^F(i/n).$$

Assumption (A2) excludes situations where $h_\alpha^F(t)$ is constant on an interval where it achieves its maximum value. This constant behavior of $h_\alpha^F(t)$ is a highly specific scenario and not easily characterized by conditions on F . (A2) also excludes cases where h_α^F is an increasing function, which can happen if the signal is too weak or the false null proportion is too large. In typical p -value models, these scenarios do not pose an issue.

Theorem 1. *Consider the p -value distribution given in (1) and assume that conditions (A1) and (A2) hold. Let $p_{(1)}, \dots, p_{(n)}$ be the order statistics of the iid sample from (1).*

Let \hat{k}_α and $\hat{\pi}_1^\alpha$ be as defined in (4) and (5), respectively, with c_n such that $\frac{nc_n}{\log \log n} \rightarrow \infty$, $\frac{\log \log(1/c_n)}{\log \log n} \rightarrow C < \infty$. It holds that

$$\hat{k}_\alpha/n \xrightarrow{a.s.} \tilde{t}_\alpha := \operatorname{argmax}_{0 \leq t \leq 1/2} \frac{F^{-1}(2t) - 2F^{-1}(t)}{t^\alpha}, \quad (7)$$

$$p_{(\hat{k}_\alpha)} \xrightarrow{a.s.} F^{-1}(\tilde{t}_\alpha), \quad (8)$$

$$\hat{\pi}_1^\alpha \xrightarrow{a.s.} \frac{\tilde{t}_\alpha - F^{-1}(\tilde{t}_\alpha)}{1 - F^{-1}(\tilde{t}_\alpha)} \leq \pi_1. \quad (9)$$

Theorem 1 explains the asymptotic behavior of the estimated change-point and the estimated proportion in terms of the ideal quantities, which are functionals of the p -value distribution quantile function. The convergence rates of the statistics in Theorem 1 are not stated here but are considered within its proof in Appendix A. These rates depend on the differentiability of h_α^F at \tilde{t}_α , and the degree of “flatness” of h_α^F at \tilde{t}_α , which is quantified using higher order derivatives.

When $\alpha_1 < \alpha_2$, the decreasing function $1/t^{\alpha_2-\alpha_1}$ implies that $\operatorname{argmax}_t h_{\alpha_1}^F(t) > \operatorname{argmax}_t h_{\alpha_2}^F(t)$. This suggests that for larger α values, the “change-point” occurs later. From Theorem 1 it also follows that the rate of convergence is slower for smaller α .

The following two corollaries follow easily from Theorem 1 and we provide them without proof. They illustrate the behavior of the proposed statistics in two specific cases.

Corollary 1 considers a special case when the p -values come from a mixture of two uniform distributions. In that case, F and F^{-1} are piecewise linear functions with one change-point where the slope changes. From Theorem 1 it follows that \hat{k}_α/n consistently estimates this change-point and that $\hat{\pi}_1^\alpha$ is an unbiased estimator of π_1 for any $\alpha \in [1/2, 1]$, with the consistency rates uniquely determined and provided in the statement.

Corollary 1. *Let $p_{(1)}, \dots, p_{(n)}$ be the order statistics of the iid sample of p -values coming from a mixture of two uniform distributions*

$$\pi_1 U[0, b] + \pi_0 U[0, 1], \quad (10)$$

where $0 < b < 1$. Let \hat{k}_α and $\hat{\pi}_1^\alpha$ be the corresponding statistics proposed in (4) and (5), respectively, with c_n such that $\frac{nc_n}{\log \log n} \rightarrow \infty$, $\frac{\log \log(1/c_n)}{\log \log n} \rightarrow C < \infty$. It holds that

$$\begin{aligned} \hat{k}_\alpha/n &\xrightarrow{a.s.} \pi_1 + b\pi_0, \\ p_{(\hat{k}_\alpha)} &\xrightarrow{a.s.} b, \\ \hat{\pi}_1^\alpha &\xrightarrow{a.s.} \pi_1. \end{aligned}$$

For large enough n , with probability one it holds that

$$\left| p_{(\hat{k}_\alpha)} - b \right| \leq C \frac{\log \log n}{nc_n^{2\alpha-1}} \quad (11)$$

$$\left| \hat{\pi}_1^{DOS} - \pi_1 \right| \leq C \frac{\log \log n}{nc_n^{2\alpha-1}}. \quad (12)$$

Thus, $p_{(\hat{k}_\alpha)}$ and $\hat{\pi}_1^\alpha$ are strongly consistent estimators of the uniform mixture parameters b and π_1 , respectively.

Corollary 2 shows that in general, when the support of the false null distribution is $[0, b]$, $p_{(\hat{k}_\alpha)}$ will a.s. not overestimate b , so $\hat{\pi}_1^\alpha$ will be a conservative estimator of the proportion.

Corollary 2. *Let $[0, b]$, $b \leq 1$ be the support of the alternative distribution F_1 , where F_1 is stochastically smaller than $U[0, b]$ distribution, in the sense that $F_1(t) \geq t/b$ for all $0 \leq t \leq b$. $p_{(\hat{k}_\alpha)}$ is an almost surely conservative estimator of the support boundary b .*

Additional remarks and discussions related to Theorem 1 can be found in Section A of the Supplementary material. Additionally, in Section B.3 of the Supplementary material, we perform a numerical examination of the asymptotic quantities defined in Theorem 1 under a specific model.

4 Simulations

In this section, we assess the performance of the DOS method by comparing it with various proportion estimators from the literature.

The choice of α impacts the estimated change-point location. As α increases, the estimated change-point location tends to occur earlier, leading to a more conservative proportion estimate on average. We conduct the simulations using $\alpha = 1/2$ and $\alpha = 1$.

The simulations in Section B.4 of the Supplementary Material show that excluding the values from the beginning of the sequence $d(i)$ does not affect the estimates. Therefore, in practice, there is no need to exclude any values when computing the estimates using the DOS method.

Below, we discuss the two simulation settings.

1. In Section 4.1, we consider the Gaussian mean testing problem, $H_0 : \mu = 0$ against $H_1 : \mu > 0$. The test statistics T_i follow a $N(0, 1)$ distribution under the null hypotheses and $N(\mu_1, 1)$ with $\mu_1 > 0$ under the alternative. One-sided p -values are calculated from the test statistics as $p_i = 1 - \Phi(T_i)$ where Φ is the standard Gaussian CDF. We compare the DOS-Storey estimator with various other proportion estimators in terms of their bias, standard deviation (SD), and root mean squared error (RMSE).
2. In Section 4.2, we consider the composite Gaussian mean testing problem, $H_0 : \mu \leq 0$ against $H_1 : \mu > 0$. The distribution under the null is $N(\mu_0, 1)$, where $\mu_0 \leq 0$ and under the alternative $N(\mu_1, 1)$ for $\mu_1 > 0$. The p -values are calculated using the least favorable parameter configuration – when μ_0 is closest to the parameter values under the alternative. This corresponds to $\mu_0 = 0$, so $p_i = 1 - \Phi(T_i)$. This setting produces superuniform p -values. The uDOS proportion estimator is compared to the method proposed in Hoang and Dickhaus (2020).

In both settings, we consider a fixed proportion of false null hypotheses. That is, for a sample of size n , and a given false null proportion π_1 , the number of false null test statistics is set to $\lfloor n\pi_1 \rfloor$. The behavior of the proposed estimators under dependence is considered in Section B.1 of the Supplementary material.

4.1 Comparison Under Uniformity

Below, we list and briefly describe the methods used in the simulation study.

1. STS – Storey and Tibshirani’s *smoother* method from Storey and Tibshirani (2003), implemented in the R package `qvalue` by Storey et al. (2020)
2. MGF – Moment Generating Function method by Broberg (2005), implemented in the R package `SAGx` by Broberg (2020)
3. LLF – Langaas-Lindqvist-Ferkingstad by Langaas et al. (2005)
4. LSL – Lowest Slope estimator by Benjamini and Hochberg (2000)
5. MR – Meinshausen-Rice by Meinshausen and Rice (2006)
6. JD – Jiang-Doerge by Jiang and Doerge (2008)
7. ST-MED – Storey’s estimator (2) with $\lambda = p_{(n/2)}$, as proposed in Benjamini et al. (2006)
8. ST-1/2 – Storey’s estimator (2) with $\lambda = 1/2$

Among the methods listed above, Storey-based methods include LSL, JD, ST-MED, and ST-1/2. LSL aims to identify the onset of the linear part and results in a conservative estimator. JD uses bootstrap and averages Storey’s proportion estimator across several λ values. The statistical literature on adaptive FDR control typically recommends using ST-1/2 (Blanchard and Roquain, 2009; Lei and Fithian, 2016; Ignatiadis and Huber, 2021). Additionally, we have LLF, a density estimation-based method, and MR, a consistent estimator constructed using the empirical processes theory. MGF is a moment generating function-based method that accounts for the behavior under the alternative. STS uses spline smoothing to combine the information from several λ values close to 1. The implementation of STS within the function `pi0est` from the R package `qvalue` is not suitable for small sample sizes and typically requires a sample size of $n \geq 200$.

The data is simulated as described at the beginning of Section 4. Table 1 provides a comparison of various proportion estimators for a sample size $n = 1000$ and different values of μ_1 and π_1 , based on $N = 1000$ repetitions. The results show that, in terms of the RMSE, DOS-Storey with $\alpha = 1$ performs better in sparse cases, whereas $\alpha = 1/2$ is better suited when there is a higher proportion of false nulls. The DOS-Storey method has a lower variance for stronger signals than the other methods (for instance, $\mu_1 = 3, \pi_1 = 0.1$ in Table 1). However, for smaller nonzero means ($\mu_1 = 2, \pi_1 = 0.1$), the objective function is smoother, increasing variability in the estimated change-point location and the proportion estimates. In general, Storey-based estimators outperform the consistent MR estimator, which significantly underestimates the false null proportion.

Simulation results for small sample sizes $n = 50$ and $n = 100$ are presented in Table 2. The STS method is excluded as it requires a larger sample size to compute the estimates. The results indicate that the two DOS-Storey estimators exhibit one of the smallest RMSE values among the considered estimators, independently of α . It remains that the DOS-1 estimator performs better in sparser cases, and the DOS-1/2 performs better in dense cases.

	DOS1	DOS05	ST-1/2	ST-MED	JD	LLF	LSL	MGF	MR	STS
$\mu_1 = 3.5, \pi_1 = 0.01, n_1 = 10$										
BIAS	<u>-0.4</u>	9.6	8.1	8.1	6.8	16.9	-3.7	3.2	-4.5	29.7
SD	3.9	15.6	22.3	21.5	21.2	22.0	<u>2.4</u>	14.2	7.0	54.0
RMSE	<u>3.9</u>	18.3	23.8	22.9	22.3	27.8	4.4	14.5	8.3	61.6
$\mu_1 = 3.5, \pi_1 = 0.03, n_1 = 30$										
BIAS	-3.0	6.3	1.8	1.5	<u>0.4</u>	15.3	-7.3	<u>-0.4</u>	-8.6	23.1
SD	5.5	13.7	26.9	25.3	26.1	21.1	<u>3.5</u>	17.3	5.6	62.2
RMSE	<u>6.3</u>	15.1	27.0	25.3	26.1	26.0	8.1	17.3	10.2	66.3
$\mu_1 = 3.0, \pi_1 = 0.05, n_1 = 50$										
BIAS	-8.9	4.3	<u>0.3</u>	0.9	-0.9	16.4	-17.5	-1.2	-16.6	18.6
SD	8.4	16.9	29.2	27.6	29.5	23.5	<u>5.4</u>	18.0	7.2	67.6
RMSE	<u>12.2</u>	17.4	29.2	27.6	29.5	28.6	18.3	18.1	18.1	70.2
$\mu_1 = 2.0, \pi_1 = 0.1, n_1 = 100$										
BIAS	-37.1	-4.6	<u>-3.6</u>	-5.0	-7.8	12.2	-67.8	-14.4	-44.9	8.9
SD	19.3	24.6	31.5	27.8	32.1	31.7	<u>9.1</u>	18.5	14.0	77.7
RMSE	41.8	25.0	31.7	28.3	33.0	33.9	68.4	<u>23.4</u>	47.0	78.2
$\mu_1 = 3.0, \pi_1 = 0.1, n_1 = 100$										
BIAS	-13.7	<u>0.5</u>	-0.6	<u>-0.5</u>	-6.0	14.6	-28.0	-2.6	-23.4	-1.1
SD	10.2	16.4	29.3	26.3	30.7	23.4	<u>7.7</u>	17.5	8.2	72.9
RMSE	17.1	<u>16.4</u>	29.3	26.4	31.2	27.6	29.1	17.6	24.8	72.9
$\mu_1 = 2.0, \pi_1 = 0.2, n_1 = 200$										
BIAS	-48.2	-17.1	-9.5	-14.9	-13.8	7.4	-117.1	-29.7	-63.7	<u>-0.3</u>
SD	26.1	23.2	28.3	22.2	30.0	32.0	<u>15.8</u>	16.8	17.4	77.3
RMSE	54.8	28.8	29.8	<u>26.7</u>	33.0	32.8	118.1	34.1	66.0	77.3
$\mu_1 = 3.0, \pi_1 = 0.2, n_1 = 200$										
BIAS	-20.4	-3.4	1.0	<u>-0.5</u>	-3.7	15.2	-44.0	-3.9	-31.7	1.3
SD	12.7	16.7	28.4	21.5	31.9	24.8	10.6	16.3	<u>10.0</u>	80.2
RMSE	24.0	<u>17.0</u>	28.4	21.5	32.1	29.1	45.2	16.8	33.3	80.2
$\mu_1 = 3.0, \pi_1 = 0.3, n_1 = 300$										
BIAS	-24.2	-6.4	-1.6	-3.4	-5.1	12.8	-53.8	-7.9	-37.6	<u>-1.0</u>
SD	13.7	14.8	25.6	16.1	30.2	23.0	14.0	14.9	<u>9.9</u>	74.6
RMSE	27.8	<u>16.1</u>	25.7	16.4	30.6	26.3	55.6	16.8	38.9	74.6

Table 1: Bias, standard deviation, and the RMSE of the estimated number of the false null hypotheses ($n \times \hat{\pi}_1$), given the proportion of false null p -values π_1 , and the non-zero mean μ_1 , for a sample of size $n = 1000$, based on 1000 repetitions. Bold and underlined values correspond to the smallest values in each row.

	DOS1	DOS05	ST-1/2	ST-MED	JD	LLF	LSL	MGF	MR
$\mu_1 = 3, \pi_1 = 0.1, n = 50$									
BIAS	0.9	2.5	0.9	1.0	0.9	3.9	-2.0	<u>0.1</u>	-3.2
SD	2.6	3.0	5.5	4.4	5.1	5.2	1.8	<u>3.5</u>	<u>1.5</u>
RMSE	2.8	3.9	5.5	4.5	5.2	6.5	<u>2.7</u>	3.5	3.5
$\mu_1 = 2, \pi_1 = 0.2, n = 50$									
BIAS	-0.9	0.9	0.2	<u>-0.1</u>	<u>0.1</u>	3.9	-4.8	-1.1	-6.4
SD	3.9	3.4	6.2	<u>4.6</u>	<u>5.7</u>	6.9	2.7	3.8	<u>2.2</u>
RMSE	4.0	<u>3.5</u>	6.2	4.6	5.7	8.0	5.5	4.0	6.8
$\mu_1 = 2, \pi_1 = 0.4, n = 50$									
BIAS	-3.0	-2.3	-0.9	-2.4	<u>-1.5</u>	2.7	-6.4	-2.9	-9.4
SD	2.8	<u>2.4</u>	5.5	2.8	<u>5.6</u>	6.5	3.8	3.5	2.6
RMSE	4.1	<u>3.3</u>	5.6	3.7	5.8	7.1	7.4	4.5	9.8
$\mu_1 = 3, \pi_1 = 0.1, n = 100$									
BIAS	0.7	3.8	1.7	1.9	1.8	5.5	-2.2	<u>0.5</u>	-3.4
SD	3.3	4.8	7.2	6.3	6.8	7.4	2.0	<u>4.7</u>	<u>1.9</u>
RMSE	3.3	6.1	7.4	6.6	7.0	9.2	<u>3.0</u>	4.7	3.9
$\mu_1 = 3, \pi_1 = 0.1, n = 100$									
BIAS	0.5	3.5	1.0	0.7	0.9	5.5	-2.8	<u>0.1</u>	-4.4
SD	3.9	4.9	8.6	7.2	7.9	7.5	2.3	<u>5.5</u>	<u>2.1</u>
RMSE	3.9	6.0	8.7	7.2	8.0	9.3	<u>3.7</u>	5.5	4.8
$\mu_1 = 2, \pi_1 = 0.2, n = 100$									
BIAS	-2.7	<u>0.3</u>	-1.0	-1.4	-1.5	4.0	-9.5	-3.0	-11.0
SD	5.9	<u>5.2</u>	8.8	6.9	8.5	8.9	4.0	5.3	<u>3.5</u>
RMSE	6.5	<u>5.2</u>	8.8	7.0	8.7	9.7	10.3	6.1	11.5
$\mu_1 = 2, \pi_1 = 0.4, n = 100$									
BIAS	-6.6	-5.2	-2.2	-5.3	<u>-2.9</u>	3.0	-14.2	-6.0	-16.3
SD	4.3	<u>3.6</u>	7.8	3.8	<u>8.1</u>	9.3	5.4	4.8	4.1
RMSE	7.9	<u>6.3</u>	8.1	6.5	8.6	9.7	15.2	7.7	16.8

Table 2: Bias, standard deviation, and the RMSE of the estimated number of the false null hypotheses ($n \times \hat{\pi}_1$), given the total number of hypotheses n , the proportion of false null hypotheses π_1 , and the non-zero mean μ_1 , based on 1000 repetitions. Bold and underlined values correspond to the smallest values in each row.

4.2 Superuniform p -values

In this section, we explore superuniform p -values generated from the composite null model introduced in Section 4. As the uniformity assumptions is violated, Storey's estimator is unsuitable. Modifications suggested in Dickhaus (2013) and Hoang and Dickhaus (2020) involve randomizing p -values to enforce uniformity and utilizing the ST-1/2 method on the randomized p -values for proportion estimation.

Under the superuniformity assumption, we propose estimating the false null proportion

directly from the change-point using the uDOS estimator defined as:

$$\hat{\pi}_{1,\text{uDOS}}^\alpha = \hat{k}_\alpha/n. \quad (13)$$

In this approach, the DOS threshold acts as a separation threshold for classifying the p -values into two groups. The estimated proportion is the proportion of values in the “small p -values group”.

We compare the performance of the uDOS estimator with the proportion estimator by Hoang and Dickhaus (2020) (HD). The data is simulated as described at the beginning of Section 4. We adopt the mean parameter values used in Hoang and Dickhaus (2020) where the mean under the null is $\mu_0 = -0.2r$ and under the alternative $\mu_1 = 1 + 0.25r$, for $r \in \{1, \dots, 10\}$. The simulations are conducted for $n = 100$ and based on $N = 10000$ repetitions.

In Figure 4, we compare the performance of the uDOS proportion estimator (13) with the estimator proposed by Hoang and Dickhaus (2020) (HD) and Storey’s estimator with $\lambda = 0.5$ applied to the non-randomized p -value sequence. In terms of the RMSE, the uDOS estimator with $\alpha = 1$ outperforms the HD method overall, although it leads to negatively biased estimates.

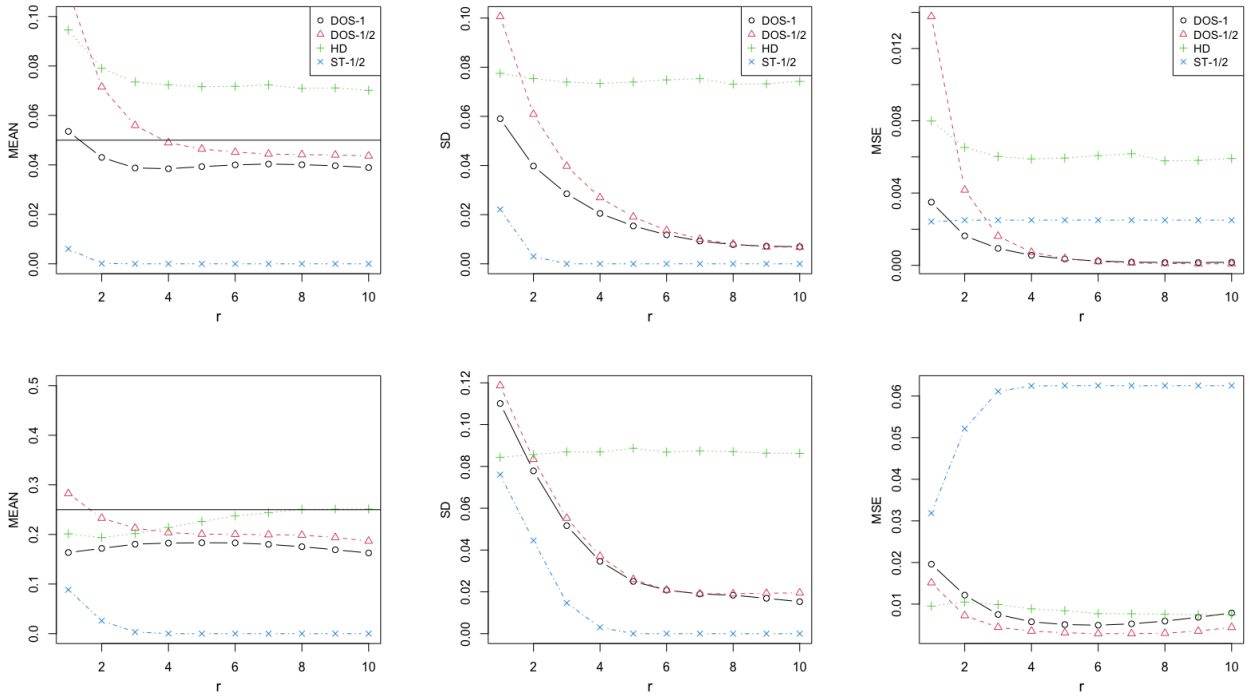


Figure 4: Mean, standard deviation, and the MSE of different proportion estimators when applied to superuniform true null p -values, generated as described in Section 4.2. The x -axis represents r , indicating the distance between the true and false null means. Top: $\pi_1 = 0.05$. Bottom: $\pi_1 = 0.25$.

5 Real Data Example

Copy Number Variations (CNVs) are genetic alterations characterized by changes in the number of copies of specific DNA segments within an individual’s genome, including duplications or deletions of these segments. These variations play a crucial role in cancer development and progression, making their detection important for understanding the genetic causes of the disease. CNV data is typically obtained through aCGH (array comparative genomic hybridization), resulting in *log ratio data*. In this data, no variation corresponds to a value of 0, while deletions are represented as decreases in value, and duplications as increases in value.

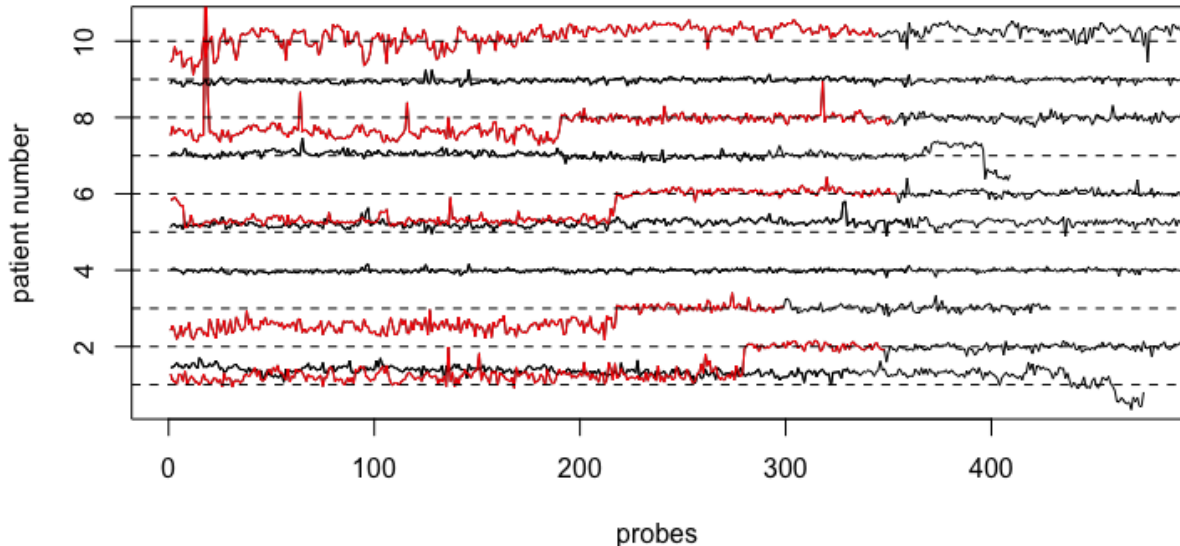


Figure 5: Log ratio data for chromosome 1, for the first ten patients.

We analyze the dataset from the R package `neuroblastoma`, which includes annotated log ratio data for 575 patients with neuroblastoma. This data is initially considered in Hocking et al. (2013). The dataset covers six chromosomes: 1, 2, 3, 4, 11, and 17. Within each chromosome, an interval of interest is examined. An expert annotates each profile as either “breakpoint” or “normal” to indicate the suspected presence of changes within that interval. CNV data for the first chromosome for the first ten patients is shown in Figure 5. The probe locations are not aligned across patients, and the x -axis shows the index of the probe for which we have available data. Deletions can be seen in profiles 2, 3, 6, and 8. We refer to these jumps in the piecewise constant mean of the profiles as breakpoints, not to be confused with the notion of change-points in the quantile function of the p -values used in the paper so far.

We explore the application of our method in the context of breakpoint inference. Our objective is to estimate the prevalence of copy number alterations (breakpoints) among these

patients, for which we propose to use the DOS-Storey method. Copy number log ratio data is usually assumed to be independent and Gaussian, with a piecewise constant underlying mean (Zhang et al., 2010; Jeng et al., 2012). However, the available data contains some outliers (see profile 8 in Figure 5), and for that reason before the analysis we trimmed the data by excluding the data points in the lower or upper 2.5th quantile. For each profile and each chromosome, a p -value arising from testing whether the profile contains a breakpoint is obtained using the method by Jewell et al. (2022). As a result we get a p -value for each patient in each of the six genomic regions. All p -values are shown in Figure 6. Note that the black bars correspond to the profiles that are annotated as “breakpoint” by the expert, however the ground truth of whether the breakpoint is present is unknown. The critical component of this analysis is the computation of p -values using the method proposed in Jewell et al. (2022). The estimation and inference on the breakpoints is performed using package `ChangepointsInference` Jewell (2023), which enables estimation of the p -values using a post-selection inference approach. A single breakpoint is estimated in each profile using the CUSUM statistic. The fixed window parameter for testing the estimated breakpoint is set to $h = 5$.

Using the DOS method with $\alpha = 1$, for each chromosome we estimate the number of profiles with breakpoints and compare it to the number of profiles annotated as having a breakpoint. We compare the estimated values to those obtained by Storey’s method with $\lambda = 0.5$ (ST-1/2). The results showing the estimated number of affected profiles for each chromosome are presented in Table 3. The values in the rightmost column (ANNOT) are the reported numbers of profiles annotated as having a breakpoint. Although the ground truth is unknown, we observe that the DOS method produces estimates that are closer to the annotated values.

	DOS-1	ST-1/2	ANNOT
Chr 1	150	167	103
Chr 2	147	146	110
Chr 3	39	70	43
Chr 4	168	195	35
Chr 11	174	243	107
Chr 17	171	193	175

Table 3: The number of affected profiles for each chromosome, estimated using the DOS-1 and ST-1/2 methods, along with the number of profiles annotated as “breakpoint” (ANNOT).

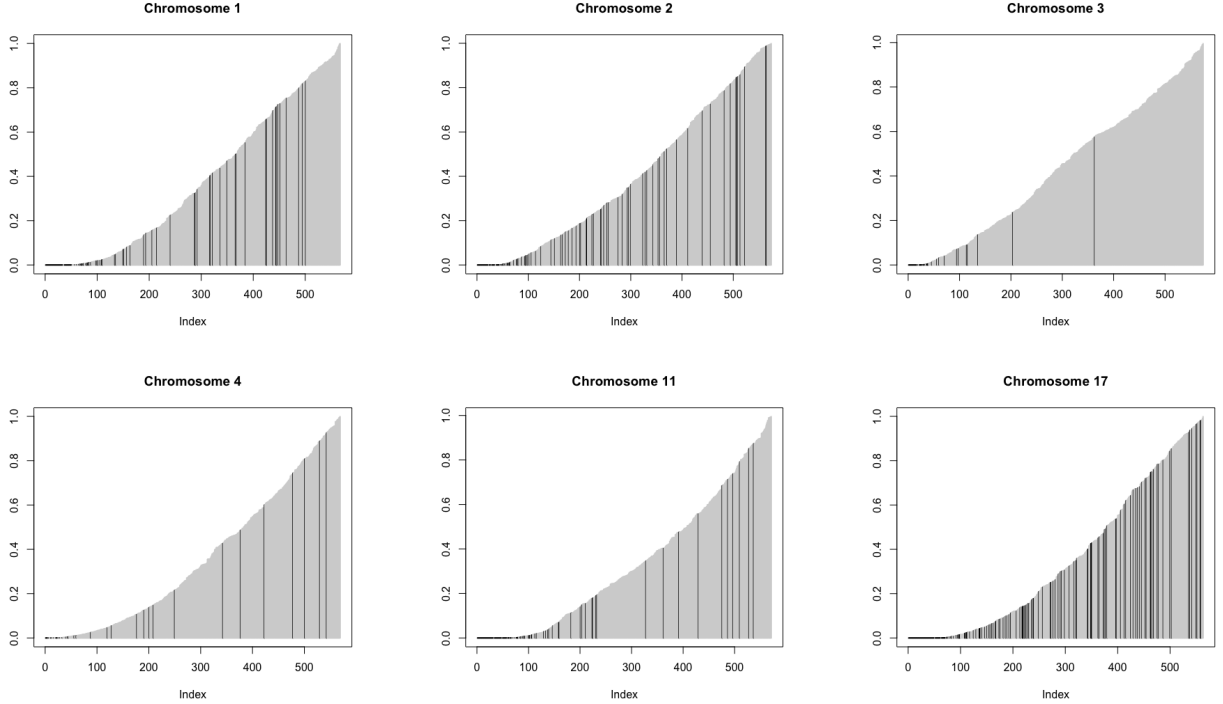


Figure 6: p -value plots for the neuroblastoma data. The black bars denote the p -values corresponding to the profiles that are annotated as “breakpoint” (with change-point in the copy number data), while the gray background corresponds to the profiles annotated as “normal” (no change in the copy number values).

Furthermore, this example motivates using multiple testing methods for estimating the subset of profiles with breakpoints in high-dimensional breakpoint problems. There is limited literature on this topic (Chen et al., 2022; Jirak, 2015; Chen et al., 2023). The existing literature typically assumes that the jumps are large enough to support theoretical statements and enable accurate estimation of the subset of affected coordinates. However, this assumption may not hold for smaller jumps, when coordinates with breakpoints might be indistinguishable from those without breakpoints. By estimating the proportion of affected profiles, our method assesses the sparsity of the high-dimensional breakpoint problem. Moreover, if selecting the subset of affected coordinates is of interest, this can be achieved using the adaptive Benjamini-Hochberg procedure, which controls the number of false discoveries.

6 Discussion

Aside from precise proportion estimation, the DOS method can be used for adaptive FDR control. Adaptive FDR control is of interest in modern multiple testing literature, where methods aim to include prior knowledge of p -values or additional assumptions about their structure. These often build on the classical BH procedure, and adaptiveness can be introduced by incorporating a proportion estimator. Some additional simulation results on the adaptive FDR control can be found in Section B.2 of the Supplementary material. The

DOS method outperforms the most commonly used proportion estimators by Benjamini and Hochberg (2000) and Storey and Tibshirani (2003) and it works well for adaptive FDR control under dependency.

The idea behind estimating a single change-point is to estimate the sparsity of the problem and divide the p -values into two categories, mostly false null, and mostly true null. For future work, it may be of interest to consider different piecewise constant approximations to the p -value spacing sequence that allow multiple change-points and, in that way, categorize p -values into multiple groups based on the decreasing frequency of the false null p -values. Grouping p -values based on their significance would provide more options for estimating the proportion at different change-points.

A Proofs

Before presenting the main theorems we state two lemmas that connect the quantile process of the p -value distribution to the uniform quantile process. This will allow us to later use some existing results on the almost sure behaviour of the weighted uniform quantile process in the proof of Theorem 1.

Notation

We denote with \hat{E}_n the empirical CDF of a sample of size n from $U[0, 1]$ distribution. The corresponding empirical and quantile processes are respectively:

$$\begin{aligned}\alpha_n(y) &= \sqrt{n}(\hat{E}_n(y) - y), \\ u_n(y) &= \sqrt{n}(\hat{E}_n^{-1}(y) - y).\end{aligned}$$

For a sample of random variables X_1, \dots, X_n with CDF F , we denote its empirical CDF as \hat{F}_n , and the corresponding quantile process as

$$q_n(y) = \sqrt{n}(\hat{F}_n^{-1}(y) - F^{-1}(y)).$$

A.1 Some Useful Lemmas

Lemma 1. *Let X_1, \dots, X_n be the sample from a distribution with CDF given as*

$$F(x) = \pi_1 F_1(x) + \pi_0 x,$$

where F_1 is a continuous weakly concave function. It holds that

$$q_n(y) \leq \frac{1}{\pi_0} u_n(y), \quad y \in (0, 1). \quad (14)$$

Proof. Let $X_{k;n}$ be the k th order statistic of the sample and let $(k-1)/n < y \leq k/n$. It

holds that

$$\begin{aligned}
q_n(y) &= \sqrt{n}(\hat{F}_n^{-1}(y) - F^{-1}(y)) \\
&= \sqrt{n}(X_{k;n} - F^{-1}(y)) \\
&= \sqrt{n}(F^{-1}(F(X_{k;n})) - F^{-1}(y)) \\
&= \sqrt{n}(F^{-1}(U_{k;n}) - F^{-1}(y)) \\
&= \sqrt{n} \frac{F^{-1}(U_{k;n}) - F^{-1}(y)}{U_{k;n} - y} (U_{k;n} - y) \\
&= \frac{F^{-1}(U_{k;n}) - F^{-1}(y)}{U_{k;n} - y} \sqrt{n}(\hat{E}_n^{-1}(y) - y) \\
&\leq \sup_{x,y} \frac{F^{-1}(y) - F^{-1}(x)}{y - x} u_n(y) \\
&\leq \frac{1}{\pi_0} u_n(y).
\end{aligned}$$

The last inequality follows from the concavity assumption as follows. As F_1 is a concave function on $[0, 1]$, and F is a linear combination of F_1 and a linear function, F is also a concave function on $[0, 1]$. It holds that the inverse of a continuous, concave and increasing function on an interval is convex on the same interval, so it follows that F^{-1} is a convex function. Since $F(x) \leq \pi_1 + \pi_0 x$ for $x \in [0, 1]$ it holds that for any $0 \leq x < y \leq 1$

$$\begin{aligned}
\frac{F^{-1}(y) - F^{-1}(x)}{y - x} &\leq \frac{1 - F^{-1}(x)}{1 - x} \\
&\leq \frac{1}{\pi_0}.
\end{aligned}$$

□

Lemma 2. *Under the assumptions of Lemma 1, it holds that*

$$P\left(\sup_{0 < y < 1} |q_n(y)| \geq x\right) \leq 2 \exp(-2x^2/C^2).$$

Proof. To prove this we use the result from Lemma 1 and the relationship between the uniform empirical and the uniform quantile process. By the change of variable argument we have $\sup_{0 < y < 1} |u_n(y)| = \sup_{0 < y < 1} |\alpha_n(y)|$ (see Remark 1.4.1 in Csörgő (1983)). The result now follows from the Dvoretzky-Kiefer-Wolfowitz inequality, using the tight bound from Massart (1990):

$$\begin{aligned}
P\left(\sup_{0 < y < 1} |q_n(y)| \geq x\right) &\leq P\left(\sup_{0 < y < 1} |u_n(y)| C \geq x\right) \\
&= P\left(\sup_{0 < y < 1} |\alpha_n(y)| \geq x/C\right) \\
&\leq 2 \exp(-2x^2/C^2).
\end{aligned}$$

□

A.2 Proof of Theorem 1

Proof. Let

$$h_n(t) := \frac{F_n^{-1}(2t) - 2F_n^{-1}(t)}{t^\alpha} \quad (15)$$

The empirical function $h_n(t)$ is approximating the ideal function $h(t)$ defined in (6) as

$$h(t) := \frac{F^{-1}(2t) - 2F^{-1}(t)}{t^\alpha}$$

For the sake of notation simplicity, we suppress the dependence of $h(t)$ and $h_n(t)$ on α and F . For the DOS sequence it holds that $d_\alpha(i) = h_n(i/n)$, for $i = 1, \dots, n$. Function h is positive on $(0, 1)$ because of the convexity assumption on F^{-1} . We start with the following sequence of inequalities, aiming to upper bound the rate of difference $|h_n(t) - h(t)|$, uniformly for $t \in (c_n, 1)$, using strong limit theorems for weighted uniform quantile processes.

$$|h_n(t) - h(t)| = \left| \frac{F_n^{-1}(2t) - 2F_n^{-1}(t)}{t^\alpha} - \frac{F^{-1}(2t) - 2F^{-1}(t)}{t^\alpha} \right| \quad (16)$$

$$\leq 2^\alpha \left| \frac{F_n^{-1}(2t) - F^{-1}(2t)}{(2t)^\alpha} \right| + 2 \left| \frac{F_n^{-1}(t) - F^{-1}(t)}{t^\alpha} \right| \quad (17)$$

$$\leq \frac{2^\alpha}{\sqrt{n}} \frac{|q_n(2t)|}{(2t)^\alpha} + \frac{2}{\sqrt{n}} \frac{|q_n(t)|}{t^\alpha} \quad (18)$$

$$\leq \frac{2^\alpha + 2}{\sqrt{n}} \sup_{t \in (c_n, 1)} \frac{|q_n(t)|}{t^\alpha} \quad (19)$$

$$\leq \frac{2^\alpha + 2}{\sqrt{n}} \frac{1}{\pi_0} \sup_{t \in (c_n, 1)} \frac{|u_n(t)|}{t^\alpha} \quad (20)$$

In the last inequality we used Lemma 1. To bound the weighted uniform quantile process we use Theorem 2 case (III) from Einmahl and Mason (1988), setting $\nu = 0$, $a_n = \log(n)/n$ using the notation therein, that describes its almost sure behaviour

$$\limsup_{n \rightarrow \infty} \sup_{c_n \leq t \leq 1} \frac{c_n^{\alpha-1/2} |u_n(t)|}{t^\alpha \sqrt{\log \log n}} \stackrel{a.s.}{=} \sqrt{2}. \quad (21)$$

meaning that, for any $\varepsilon > 0$ and large enough n , on a set of probability 1, it holds that

$$\frac{1}{\sqrt{n}} \sup_{c_n \leq t \leq 1} \frac{|u_n(t)|}{t^\alpha} \leq \frac{\sqrt{\log \log n}}{\sqrt{n} c_n^{\alpha-1/2}} (\sqrt{2} + \varepsilon) \quad (22)$$

Finally, (22) and (20) give a uniform upper bound for $|h_n(t) - h(t)|$ on $t \in (c_n, 1]$

$$\sup_{t \in (c_n, 1]} |h_n(t) - h(t)| \leq C \frac{\sqrt{\log \log n}}{\sqrt{n} c_n^{\alpha-1/2}}, \quad (23)$$

where C is a constant that for large n approaches $\sqrt{2}$. Denote

$$\begin{aligned} \hat{t}_n^d &:= \frac{1}{n} \operatorname{argmax}_{1 \leq i \leq n} d(i) & \hat{t}_n &:= \operatorname{argsup}_{t \in [0, 1]} h_n(t) \\ \tilde{t}_n^d &:= \frac{1}{n} \operatorname{argmax}_{1 \leq i \leq n} h(i/n) & \tilde{t} &:= \operatorname{argmax}_{t \in [0, 1]} h(t) \end{aligned}$$

Since \tilde{t}_n^d is the argmax of a continuous function on an increasingly dense grid, it holds that $|\tilde{t}_n^d - \tilde{t}| \leq 1/n$. Since h is bounded and continuous on $[0, 1]$, it follows that for some $C' > 0$ $|h(\tilde{t}_n^d) - h(\tilde{t})| \leq C'/n$. For n large enough, $\tilde{t} > c_n$, the following sequence of inequalities holds with probability 1.

$$\begin{aligned} h(\tilde{t}) &\leq h(\tilde{t}_n^d) + C'/n \\ &\leq |h_n(\tilde{t}_n^d)| + C \frac{\sqrt{\log \log n}}{\sqrt{n}c_n^{\alpha-1/2}} + C'/n \\ &\leq |h_n(\hat{t}^d)| + C_1 \frac{\sqrt{\log \log n}}{\sqrt{n}c_n^{\alpha-1/2}} \\ &\leq h(\hat{t}^d) + 2C_1 \frac{\sqrt{\log \log n}}{\sqrt{n}c_n^{\alpha-1/2}}, \end{aligned}$$

where C_1 gets arbitrarily close to $\sqrt{2}$. It implies

$$h(\tilde{t}) - h(\hat{t}^d) \leq 2C_1 \frac{\sqrt{\log \log n}}{\sqrt{n}c_n^{\alpha-1/2}} \quad (24)$$

We prove the consistency of \hat{t}^d by contradiction. However, the rate of convergence depends on the differentiability of h , and we separate three different cases.

Case 1: h has a second derivative at \tilde{t} , and $h''(\tilde{t}) \neq 0$.

Case 2: h has a second derivative at \tilde{t} , and $h''(\tilde{t}) = 0$.

Case 3: h does not have a second derivative at \tilde{t} .

We start with Case 1, and note that a sufficient condition for h to be twice differentiable is that F is twice differentiable on $(0, 1)$. Assuming that $|\hat{t}^d - \tilde{t}| > \frac{\sqrt{\log \log n}}{\sqrt{n}c_n^{\alpha-1/2}}$, it holds that

$$\begin{aligned} |h(\tilde{t}) - h(\hat{t}^d)| &= (\hat{t}^d - \tilde{t})^2 |h''(\tilde{t})| + o((\hat{t}^d - \tilde{t})^2) \\ &\geq C_2 \frac{\log \log n}{\sqrt{n}c_n^{\alpha-1/2}}. \end{aligned}$$

For large n , the last inequality is in contradiction with (24), so it must hold that

$$|\hat{t}^d - \tilde{t}| \leq \frac{\sqrt{\log \log n}}{\sqrt{n}c_n^{\alpha-1/2}}, \quad (25)$$

which proves the consistency in (7). For Case 2, if $h''(\tilde{t}) = 0$, the consistency still holds, since not all derivatives can be zero, but the rate of convergence is slower accordingly. In Case 3, when h is not differentiable at \tilde{t} , such that left and right derivatives at \tilde{t} are not equal, but lower bounded by a constant larger than zero in an interval around \tilde{t} , we can get a better convergence rate:

$$|\hat{t}^d - \tilde{t}| \leq C \frac{\log \log n}{nc_n^{2\alpha-1}}.$$

This is the case for example when F is a mixture of uniform distributions (see Corollary 1). In other cases, we similarly have (25) to hold. We proceed under Case 1, assuming that $h''(\tilde{t}) \neq 0$ holds, while the results for other cases can be obtained similarly. The following sequence of inequalities holds almost surely and proves the almost sure convergence in (8):

$$\begin{aligned}
\left| p_{(\hat{k}_\alpha)} - F^{-1}(\tilde{t}) \right| &= \left| \hat{F}_n^{-1}(\hat{t}^d) - F^{-1}(\tilde{t}) \right| \\
&\leq \left| \hat{F}_n^{-1}(\hat{t}^d) - F^{-1}(\hat{t}^d) \right| + \left| F^{-1}(\hat{t}^d) - F^{-1}(\tilde{t}) \right| \\
&\leq C_3 \sqrt{\frac{\log \log n}{n}} + C_4 \sqrt{\frac{\log \log n}{nc_n^{2\alpha-1}}} \\
&\leq C_5 \sqrt{\frac{\log \log n}{nc_n^{2\alpha-1}}}.
\end{aligned} \tag{26}$$

For the first term in (26) we use Lemma 1 and then the Chung-Smirnov law of iterated logarithm, to get the inequality which holds almost surely. For the second term we use the fact that F^{-1} is Lipschitz continuous, and the obtained rate of convergence in (25). The convergence in (9) follows similarly:

$$\begin{aligned}
\left| \hat{\pi}_1^{DOS} - \frac{\tilde{t} - F^{-1}(\tilde{t})}{1 - F^{-1}(\tilde{t})} \right| &= \left| \frac{\hat{t}^d - F^{-1}(\hat{t}^d)}{1 - F^{-1}(\hat{t}^d)} - \frac{\tilde{t} - F^{-1}(\tilde{t})}{1 - F^{-1}(\tilde{t})} \right| \\
&\leq \left| \frac{(1 - F^{-1}(\hat{t}^d))(\hat{t}^d - \tilde{t}) + \hat{t}^d(F^{-1}(\hat{t}^d) - F^{-1}(\tilde{t}))}{(1 - F^{-1}(\tilde{t}))(1 - F^{-1}(\hat{t}^d))} \right| \\
&\leq C_6 \sqrt{\frac{\log \log n}{n^{\frac{1-\theta}{2}}}}.
\end{aligned}$$

□

Remark 1. The conditions on c_n in Theorem 1 come from the theorem in Einmahl and Mason (1988). Instead of $c_n \rightarrow 0$, we can trivially take $c_n = \varepsilon \in (0, 1)$, in which case we can simply use the Chung-Smirnov law stated in the proof of Theorem 1, to get the rate of convergence of $\frac{\sqrt{\log \log n}}{\sqrt{n}}$. From the work of Einmahl and Mason (1988) we see that the choice of c_n is very important in the theory of uniform quantile processes. As the false-null distribution F_1 is unknown, using the result from Lemma 2 we bound the quantile process of distribution F by a uniform quantile process. This approximation is convenient as most of the results in the theory of quantile processes are given only for the uniform quantile process. However, the behaviour of the weighted uniform quantile process around 0 will be more variable than that of weighted quantile process of a distribution F . F is more concentrated around zero and the sample quantiles will be closer to the true quantiles than in the case of uniform distribution, which reduces the boundary problem.

References

- Benjamini, Y. and Hochberg, Y. (1995). Controlling the False Discovery Rate: A Practical and Powerful Approach to Multiple Testing. *Journal of the Royal Statistical Society: Series B*, 57, 289–300.
- Benjamini, Y. and Hochberg, Y. (2000). On the Adaptive Control of The False Discovery Rate in Multiple Testing With Independent Statistics. *Journal of Educational and Behavioral Statistics*, 25, 60–83.
- Benjamini, Y., Krieger, A. M., and Yekutieli, D. (2006). Adaptive Linear Step-Up Procedures That Control the False Discovery Rate. *Biometrika*, 93, 491–507.
- Blanchard, G., Lee, G., and Scott, C. (2010). Semi-Supervised Novelty Detection. *Journal of Machine Learning Research*, 11(99), 2973–3009.
- Blanchard, G. and Roquain, É. (2009). Adaptive False Discovery Rate Control Under Independence and Dependence. *Journal of Machine Learning Research*, 10, 2837–2871.
- Broberg, P. (2005). A Comparative Review of Estimates of the Proportion Unchanged Genes and the False Discovery Rate. *BMC Bioinformatics*, 6, 199.
- Broberg, P. (2020). *SAGx: Statistical Analysis of the GeneChip*. R package version 1.64.0.
- Brodsky, B. E. and Darkhovsky, B. S. (1993). *Nonparametric Methods in Change-Point Problems*. Springer Dordrecht.
- Cai, T. T., Jin, J., and Low, M. G. (2007). Estimation and Confidence Sets for Sparse Normal Mixtures. *The Annals of Statistics*, 35, 2421–2449.
- Celisse, A. and Robin, S. (2010). A Cross-Validation Based Estimation of the Proportion of True Null Hypotheses. *Journal of Statistical Planning and Inference*, 140, 3132–3147.
- Chen, L., Wang, W., and Wu, W. B. (2022). Inference of Breakpoints in High-dimensional Time Series. *Journal of the American Statistical Association*, 117, 1951–1963.
- Chen, Y., Wang, T., and Samworth, R. J. (2023). Inference in High-Dimensional Online Changepoint Detection. *Journal of the American Statistical Association*, pages 1–12.
- Csörgő, M. (1983). *Quantile Processes With Statistical Applications*. Society for Industrial and Applied Mathematics.
- Cuomo, A. S. E., Seaton, D. D., McCarthy, D. J., Martinez, I., Bonder, M. J., Garcia-Bernardo, J., Amatya, S., Madrigal, P., Isaacson, A., Buettner, F., Knights, A., Natarajan, K. N., et al. (2020). Single-Cell RNA-Sequencing of Differentiating iPS Cells Reveals Dynamic Genetic Effects on Gene Expression. *Nature Communications*, 11, 810.
- Dickhaus, T. (2013). Randomized p-Values for Multiple Testing of Composite Null Hypotheses. *Journal of Statistical Planning and Inference*, 143, 1968–1979.

- Einmahl, J. H. J. and Mason, D. M. (1988). Strong Limit Theorems for Weighted Quantile Processes. *The Annals of Probability*, 16, 1623–1643.
- Genovese, C. and Wasserman, L. (2004). A Stochastic Process Approach to False Discovery Control. *The Annals of Statistics*, 32, 1035–1061.
- Gigante, C. M., Korber, B., Seabolt, M. H., Wilkins, K., Davidson, W., Rao, A. K., Zhao, H., Smith, T. G., Hughes, C. M., Minhaj, F., Waltenburg, M. A., et al. (2022). Multiple Lineages of Monkeypox Virus Detected in the United States, 2021–2022. *Science*, 378, 560–565.
- Hoang, A.-T. and Dickhaus, T. (2020). On the Usage of Randomized p-Values in the Schweder–Spjøtvoll Estimator. *Annals of the Institute of Statistical Mathematics*, 74, 289–319.
- Hocking, T. D., Schleiermacher, G., Janoueix-Lerosey, I., Boeva, V., Cappel, J., Delattre, O., Bach, F., and Vert, J.-P. (2013). Learning Smoothing Models of Copy Number Profiles Using Breakpoint Annotations. *BMC Bioinformatics*, 14, 164.
- Hwang, Y. T., Kuo, H. C., Wang, C. C., and Lee, M. F. (2014). Estimating the Number of True Null Hypotheses in Multiple Hypothesis Testing. *Statistics and Computing*, 24, 399–416.
- Ignatiadis, N. and Huber, W. (2021). Covariate Powered Cross-Weighted Multiple Testing. *Journal of the Royal Statistical Society: Series B*, 83, 720–751.
- Jain, S., White, M., and Radivojac, P. (2016). Estimating the class prior and posterior from noisy positives and unlabeled data. In *Advances in Neural Information Processing Systems*, volume 29.
- Jain, S., White, M., and Radivojac, P. (2017). Recovering true classifier performance in positive-unlabeled learning. In *Proceedings of the AAAI Conference on Artificial Intelligence*, volume 31.
- Jeng, X. J., Cai, T. T., and Li, H. (2012). Simultaneous Discovery of Rare and Common Segment Variants. *Biometrika*, 100, 157–172.
- Jewell, S. (2023). *ChangepointInference: Testing for a Change in Mean After Changepoint Detection*. R package version 0.9.
- Jewell, S., Fearnhead, P., and Witten, D. (2022). Testing for a Change in Mean after Changepoint Detection. *Journal of the Royal Statistical Society: Series B*, 84, 1082–1104.
- Jiang, H. and Doerge, R. (2008). Estimating the Proportion of True Null Hypotheses for Multiple Comparisons. *Cancer Informatics*, 6, 25–32.
- Jirak, M. (2015). Uniform Change Point Tests in High Dimension. *The Annals of Statistics*, 43, 2451–2483.

- Klunk, J., Vilgalys, T. P., Demeure, C. E., Cheng, X., Shiratori, M., Madej, J., Beau, R., Elli, D., Patino, M. I., Redfern, R., DeWitte, S. N., et al. (2022). Evolution of Immune Genes is Associated With the Black Death. *Nature*, 611, 312–319.
- Langaas, M., Lindqvist, B. H., and Ferkingstad, E. (2005). Estimating the Proportion of True Null Hypotheses, With Application to DNA Microarray Data. *Journal of the Royal Statistical Society: Series B*, 67, 555–572.
- Legut, M., Gajic, Z., Guarino, M., Daniloski, Z., Rahman, J. A., Xue, X., Lu, C., Lu, L., Mimitou, E. P., Hao, S., et al. (2022). A Genome-Scale Screen for Synthetic Drivers of T Cell Proliferation. *Nature*, 603, 728–735.
- Lei, L. and Fithian, W. (2016). Power of Ordered Hypothesis Testing. In *Proceedings of The 33rd International Conference on Machine Learning*, volume 48.
- Massart, P. (1990). The Tight Constant in the Dvoretzky-Kiefer-Wolfowitz Inequality. *The Annals of Probability*, 18, 1269–1283.
- Meinshausen, N. and Rice, J. (2006). Estimating the Proportion of False Null Hypotheses Among a Large Number of Independently Tested Hypotheses. *Annals of Statistics*, 34, 373–393.
- Patra, R. K. and Sen, B. (2016). Estimation of a Two-Component Mixture Model With Applications to Multiple Testing. *Journal of the Royal Statistical Society: Series B*, 78, 869–893.
- Pounds, S. and Morris, S. W. (2003). Estimating the Occurrence of False Positives and False Negatives in Microarray Studies by Approximating and Partitioning the Empirical Distribution of p-Values. *Bioinformatics*, 19, 1236–1242.
- Schweder, T. and Spjøtvoll, E. (1982). Plots of p-values to Evaluate Many Tests Simultaneously. *Biometrika*, 69, 493–502.
- Storey, J. D. (2002). A Direct Approach to False Discovery Rates. *Journal of the Royal Statistical Society: Series B*, 64, 479–498.
- Storey, J. D., Bass, A. J., Dabney, A., and Robinson, D. (2020). *qvalue: Q-value Estimation for False Discovery Rate Control*. R package version 2.22.0.
- Storey, J. D., Taylor, J. E., and Siegmund, D. (2004). Strong Control, Conservative Point Estimation and Simultaneous Conservative Consistency of False Discovery Rates: A Unified Approach. *Journal of the Royal Statistical Society: Series B*, 66, 187–205.
- Storey, J. D. and Tibshirani, R. (2003). Statistical Significance for Genomewide Studies. *Proceedings of the National Academy of Sciences*, 100, 9440–9445.
- Swanepoel, J. W. (1999). The Limiting Behavior of a Modified Maximal Symmetric 2s-spacing With Applications. *The Annals of Statistics*, 27, 24–35.

- Taquet, M., Smith, S. M., Prohl, A. K., Peters, J. M., Warfield, S. K., Scherrer, B., and Harrison, P. J. (2021). A Structural Brain Network of Genetic Vulnerability to Psychiatric Illness. *Molecular Psychiatry*, 26, 2089–2100.
- Turkheimer, F. E., Smith, C. B., and Schmidt, K. (2001). Estimation of The Number of “True” Null Hypotheses in Multivariate Analysis of Neuroimaging Data. *NeuroImage*, 13, 920–930.
- Wittenbecher, C., Guasch-Ferré, M., Haslam, D. E., Dennis, C., Li, J., Bhupathiraju, S. N., Lee, C.-H., Qi, Q., Liang, L., Eliassen, A. H., Clish, C., Sun, Q., and Hu, F. B. (2022). Changes in Metabolomics Profiles Over Ten Years and Subsequent Risk of Developing Type 2 Diabetes: Results From The Nurses’ Health Study. *eBioMedicine*, 75, 103799.
- Xu, H., Di Antonio, M., McKinney, S., Mathew, V., Ho, B., O’Neil, N. J., Santos, N. D., Silvester, J., Wei, V., Garcia, J., Kabeer, F., et al. (2017). CX-5461 is a DNA G-Quadruplex Stabilizer With Selective Lethality in BRCA1/2 Deficient Tumours. *Nature Communications*, 8, 14432.
- Zhang, N. R., Siegmund, D. O., Ji, H., and Li, J. Z. (2010). Detecting Simultaneous Change-points in Multiple Sequences. *Biometrika*, 97, 631–645.

Supplementary Material for “A Change-Point Approach to Estimating the Proportion of False Null Hypotheses in Multiple Testing”

Anica Kostic^{*†}

Piotr Fryzlewicz,[†]

This supplement provides further insights into the theoretical properties of the proposed method and presents additional simulation results. We outline the sections as follows:

- In Section A, we extend the discussion by stating a few remarks regarding Theorem 1.
- Section B contains various additional simulation results. Namely, it involves:
 1. Additional simulation results under dependence in Section B.1
 2. Comparison of various proportion estimators for adaptive FDR control using the adaptive BH procedure in Section B.2.
 3. Numerical results on the limiting behavior of the proposed statistics under the Gaussian model done in Mathematica in Section B.3.
 4. Simulation results examining the sensitivity of the DOS method with respect to c_n , the proportion of excluded values, in Section B.4.
- Section C contains additional discussion on the meaning of the DOS statistic.

A Theoretical Remarks

Remark 1. Examples can be constructed for which the assumption (A2) does not hold. First, if the signal is too weak, Q does not have a prominent change-point, which results in h increasing on $[0, 0.5]$. An illustration of this can be seen in Figure 1. Another requirement of (A2) is that h achieves a single local (and global) maximum within the interval $(0, 0.5)$. This requirement can be violated if h is constant on an interval where it achieves its maximum value. We illustrate this by taking a p -value distribution to be a uniform mixture distribution whose quantile function is piecewise linear with change-points in slope at 0.1, 0.2, 0.3, 0.4 and with increasing slopes on the first four segments equal to 0.1, 0.2, 0.4, 0.9. The corresponding function $h(t)$ is constant on the interval $[0.3, 0.4]$ where its value is maximal. This example is shown in Figure 2.

^{*}Author for correspondence. [E-mail: a.kostic@lse.ac.uk, Address: Department of Statistics, London School of Economics and Political Science, Columbia House, Houghton Street, London, WC2A 2AE, UK]

[†]London School of Economics and Political Science

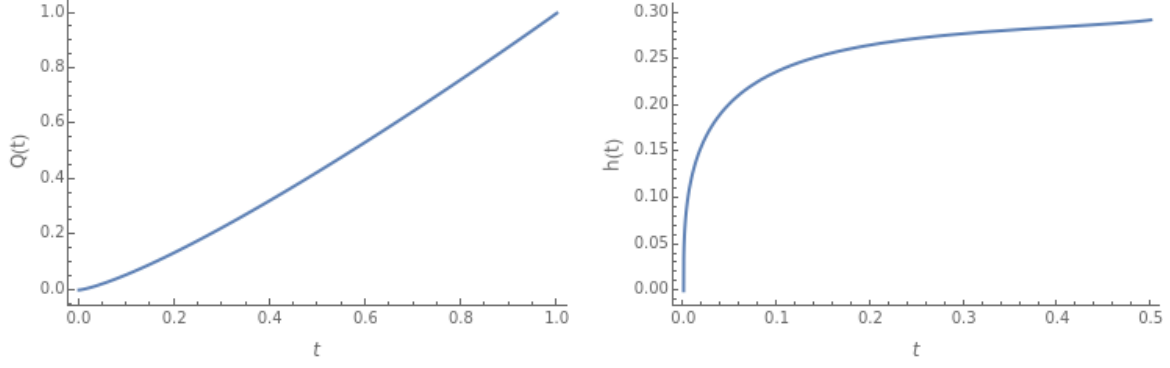


Figure 1: An example where assumption (A2) from the main paper is violated as h increases over $[0, 0.5]$. Left: Quantile function of p -values from the Gaussian model with $\pi_1 = 0.2$ and $\mu = 1$. Right: Corresponding h function.

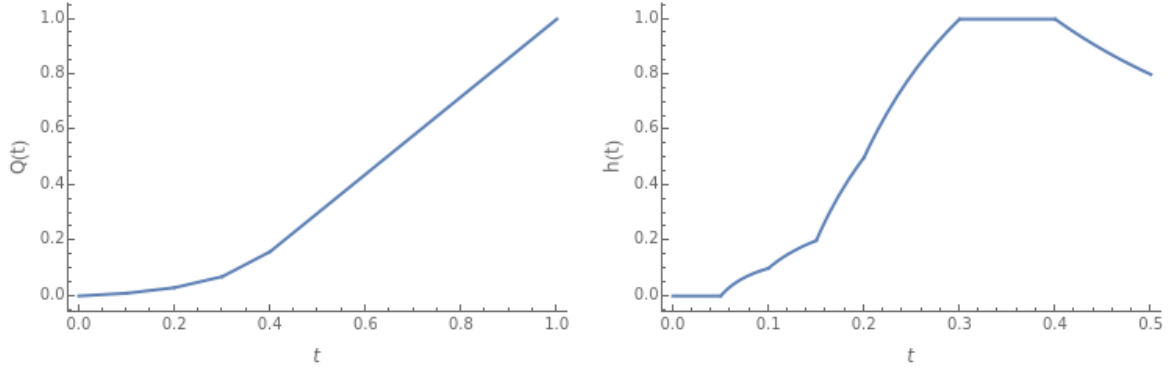


Figure 2: An example illustrating the violation of assumption (A2) from the main paper. The p -values distribution is modeled as a mixture of several uniforms. Left: Quantile function of the uniform mixture. Right: The function h is constant on $[0.3, 0.4]$ where it reaches its maximum value.

Remark 2. Although Theorem 1 is formulated for when the true null p -values distribution is uniform, it can be applied for other mixtures F . For example, let $F(x) = \pi_1 F_1(x) + \pi_0 F_0(x)$, $0 \leq x \leq 1$, where F_0 is a continuous superuniform distribution on $[0, 1]$ and F_1 is a concave CDF of a continuous distribution under the alternative that is stochastically smaller than $U[0, 1]$. Assumption (A1) might not hold in that case, which affects the result of Lemma 1. Specifically, the convexity assumption was used in Lemma 1 to bound $\sup_{x,y} \frac{F^{-1}(y) - F^{-1}(x)}{y - x}$. This expression is still finite, which yields $|q_n(y)| \leq C|u_n(y)|$, although the constant C may not be equal to $1/\pi_0$ as in Lemma 1. Note that C can get very large if F_0 and F_1 are very well separated, implying that F^{-1} very steep. In addition, if assumption (A2) holds, Theorem 1 can be applied to determine the asymptotic behavior of the uDOS estimator. Asymptotically, the uDOS proportion estimator then converges to the ideal change-point location, which is the proposed separation threshold:

$$\hat{\pi}_{1,\text{uDOS}}^\alpha \rightarrow \operatorname{argmax}_{0 \leq t \leq 1/2} \frac{F^{-1}(2t) - 2F^{-1}(t)}{t^\alpha}, \quad n \rightarrow \infty. \quad (1)$$

B Additional Simulations

B.1 Dependent p -values

This section provides simulation results of the DOS-Storey and the uDOS estimators under dependence. We now describe the model used to generate the p -values, similar to the Gaussian mean testing described in Section 4 of the main paper, but incorporating dependence in the p -value sequence. The test statistics are $T_i = \mu + \varepsilon_i$, where μ is the mean parameter of the Gaussian distribution we are testing. Under the null hypothesis $\mu = 0$ and under the alternative $\mu > 0$. Random variables ε_i are defined as

$$\varepsilon_i = \sqrt{\rho}U_i + \sqrt{1-\rho}Z_i. \quad (2)$$

where U_i and Z_i are iid $N(0, 1)$ random variables and $\rho \in [0, 1]$ is a correlation parameter. For $\rho > 0$ this introduces positive correlation in the test statistics, $\text{corr}(T_i, T_j) = \rho$, for $i \neq j$. The p -values are calculated as $p_i = 1 - \Phi(T_i)$. The simulation results are based on the sample size $n = 100$ and various values for the mean under the alternative and various π_0 values. The number of repetitions is $N = 1000$.

The simulation results for $\rho = 0.2$ are shown in Table 1 and for $\rho = 0.5$ in Table 2. Both tables show that DOS-Storey methods perform well compared to other methods in the presence of dependence.

We also include simulations under dependence for superuniform p -values. We adopt the simulation setting used in Hoang and Dickhaus (2020). The mean under the null is $\mu_0 = -0.2r$ and under the alternative $\mu_1 = 1 + 0.25r$ for $r \in \{1, \dots, 10\}$. The correlation is introduced as in 2 and the p -values are calculated as $p_i = 1 - \Phi(T_i)$. All the simulations are conducted for $n = 100$. In Figure 3, we illustrate the performance of the uncorrected DOS proportion estimator under dependence alongside the estimator proposed by Hoang and Dickhaus (2020) (HD). We show the estimators' average mean, standard deviation, and RMSE based on $N = 10000$ repetitions. The results are similar to the independent case discussed in the main paper. Both DOS-Storey estimates have negative bias but uniformly smaller MSE than the HD estimates.

Note that although the RMSE of the DOS estimator is smaller than that of the HD, the unbiasedness of the HD estimator plays a more significant role in adaptive FDR control, resulting in more accurate FDR control.

	DOS1	DOS05	ST-1/2	ST-MED	JD	LLF	LSL	MGF	MR
$\mu = 3, \pi_1 = 0.05$									
BIAS	4.60	7.90	12.90	7.30	15.10	24.50	<u>-0.60</u>	89.30	4.30
SD	12.60	13.00	22.30	13.70	22.70	32.90	<u>8.20</u>	1143.10	14.80
RMSE	13.40	15.30	25.80	15.60	27.30	41.00	<u>8.20</u>	1146.60	15.40
$\mu = 2, \pi_1 = 0.1$									
BIAS	1.50	3.90	8.60	3.00	11.40	20.70	-4.80	4.50	<u>-0.80</u>
SD	13.40	13.20	22.40	14.00	23.30	32.70	<u>9.50</u>	16.70	14.70
RMSE	13.40	13.70	24.00	14.30	26.00	38.70	<u>10.60</u>	17.40	14.80
$\mu = 3, \pi_1 = 0.1$									
BIAS	2.40	4.10	7.60	2.20	9.30	17.50	-2.40	3.70	<u>0.10</u>
SD	11.90	12.20	23.10	14.10	22.90	30.20	<u>10.60</u>	17.00	14.40
RMSE	<u>12.10</u>	12.90	24.40	14.20	24.70	34.90	10.80	17.40	14.40
$\mu = 2, \pi_1 = 0.2$									
BIAS	-2.30	-0.70	5.00	-2.10	6.70	15.90	-9.10	<u>0.20</u>	-6.50
SD	14.20	13.90	24.80	15.20	25.00	32.20	<u>12.60</u>	18.80	16.20
RMSE	14.40	<u>13.90</u>	25.30	15.40	25.90	35.90	15.60	18.80	17.40
$\mu = 3, \pi_1 = 0.2$									
BIAS	<u>0.60</u>	2.20	4.50	-1.40	6.30	17.30	-4.30	1.60	-3.50
SD	10.40	10.40	22.50	14.30	22.90	27.80	<u>9.10</u>	17.40	12.40
RMSE	10.40	10.60	22.90	14.40	23.80	32.70	<u>10.00</u>	17.40	12.90
$\mu = 3, \pi_1 = 0.3$									
BIAS	-2.10	-0.70	<u>-0.40</u>	-6.00	1.80	13.30	-5.20	-1.70	-6.50
SD	10.00	<u>9.70</u>	24.90	15.50	25.80	26.80	12.40	19.70	13.10
RMSE	10.20	<u>9.80</u>	24.90	16.60	25.90	29.90	13.40	19.70	14.60

Table 1: Simulations under dependence, where p -values follow the model described in Section B.1 with $\rho = 0.2$. Bias, standard deviation, and the RMSE of the estimated number of the false null hypotheses ($n \times \hat{\pi}_1$), given the proportion of false null p -values π_1 , and the non-zero mean μ_1 , for a sample of size $n = 100$, based on 1000 repetitions. Bold and underlined values correspond to the smallest values in each row.

	DOS1	DOS05	ST-1/2	ST-MED	JD	LLF	LSL	MGF	MR
$\mu = 3, \pi_1 = 0.05$									
BIAS	5.1	9.1	23.4	10.0	26.7	38.0	<u>4.7</u>	772.2	15.6
SD	16.3	17.0	34.0	16.8	34.4	44.0	25.5	3850.2	24.3
RMSE	<u>17.0</u>	19.3	41.2	19.5	43.5	58.2	25.9	3926.9	28.9
$\mu = 2, \pi_1 = 0.1$									
BIAS	1.2	3.8	18.0	4.9	21.8	34.6	<u>0.1</u>	516.0	10.4
SD	17.1	17.0	33.2	16.6	34.2	44.0	24.6	4331.4	24.0
RMSE	<u>17.1</u>	17.4	37.8	17.3	40.6	56.0	24.6	4362.0	26.2
$\mu = 3, \pi_1 = 0.1$									
BIAS	<u>1.0</u>	3.1	14.6	3.5	18.1	27.5	<u>1.0</u>	2184.0	7.7
SD	<u>15.7</u>	16.3	32.9	16.7	33.4	42.6	25.0	19327.1	23.8
RMSE	<u>15.7</u>	16.6	36.0	17.0	38.0	50.8	25.0	19450.1	25.0
$\mu = 2, \pi_1 = 0.2$									
BIAS	-4.8	-2.3	12.1	-2.0	16.0	28.1	-5.3	2364.8	2.0
SD	18.2	<u>17.7</u>	34.8	<u>17.7</u>	35.1	43.4	27.4	21655.1	25.1
RMSE	18.8	17.9	36.8	<u>17.8</u>	38.5	51.7	27.9	21783.8	25.2
$\mu = 3, \pi_1 = 0.2$									
BIAS	-2.1	-0.6	11.1	-1.9	15.9	28.3	-4.5	310.3	2.6
SD	<u>15.1</u>	15.3	32.6	17.0	33.6	41.3	21.3	2728.7	23.4
RMSE	<u>15.3</u>	<u>15.3</u>	34.4	17.1	37.2	50.0	21.8	2746.3	23.5
$\mu = 3, \pi_1 = 0.3$									
BIAS	-6.8	-5.7	<u>4.2</u>	-9.2	8.3	19.6	-7.1	32.6	-4.6
SD	15.2	<u>15.1</u>	34.6	18.4	35.4	39.8	24.6	466.3	24.4
RMSE	16.7	<u>16.2</u>	34.9	20.6	36.3	44.4	25.6	467.4	24.8

Table 2: Simulations under dependence, where p -values follow the model described in Section B.1 with $\rho = 0.5$. Bias, standard deviation, and the RMSE of the estimated number of the false null hypotheses ($n \times \hat{\pi}_1$), given the proportion of false null p -values π_1 , and the non-zero mean μ_1 , for a sample of size $n = 100$, based on 1000 repetitions. Bold and underlined values correspond to the smallest values in each row.

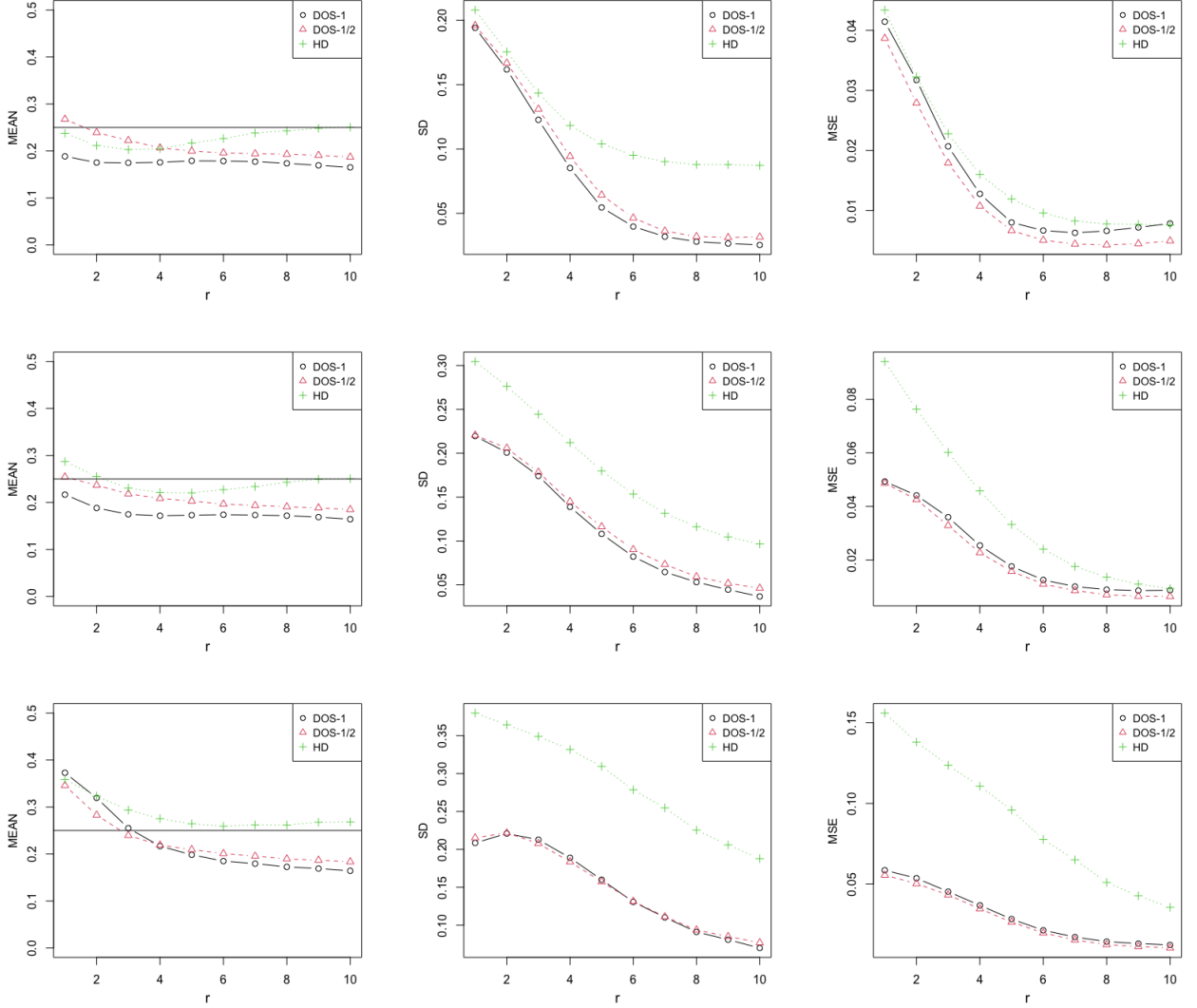


Figure 3: Mean, standard deviation, and the MSE of different proportion estimators when applied to superuniform true null p -values, generated as described in Section B.1. The x -axis represents r , indicating the distance between the true and false null means. From top to bottom: correlation coefficient $\rho \in \{0.25, 0.5, 0.75\}$.

B.2 Adaptive FDR Control

In this section, we illustrate the performance of the DOS-Storey proportion estimator for adaptive FDR control. We evaluate its performance under dependence and independence and compare it to adaptive procedures using different estimators.

The FDR-controlling multiple testing procedure proposed by Benjamini and Hochberg (1995) (BH) rejects the hypotheses corresponding to the \hat{k} smallest p -values, where $\hat{k} = \max \{k \geq 1 : p_{(k)} \leq \alpha \frac{k}{n}\}$ and $p_{(1)} \leq \dots \leq p_{(n)}$. It achieves effective FDR control at level $\pi_0 \alpha$. As suggested by Benjamini and Hochberg (2000), incorporating a proportion estimator into the BH procedure increases its power by adapting to the unknown proportion. This

adaptation is achieved by increasing the FDR level parameter from α to $\alpha' = \alpha/\hat{\pi}_0$, which results in a higher number of rejections while maintaining approximate FDR control at level α . The simulation study in this section investigates how different proportion estimators affect FDR control and the power of the resulting adaptive procedures. In the context of an adaptive BH procedure, power is defined as the ratio of the number of true discoveries to the total number of false null hypotheses. Note that in this section, we use α to refer to the level of the FDR control and not the parameter of the DOS sequence from the main paper.

Since the DOS method is unsuitable when the false null proportion is very large, we restrict our analysis to cases where $\pi_0 \geq 0.5$ ($\pi_1 \leq 0.5$). We adopt the simulation settings used in Blanchard and Roquain (2009). We consider various values for the mean under the alternative and various π_0 values. The desired level of the FDR control is set to $\alpha = 0.05$. Figures 4 and 5 show the simulation results of this analysis for sample size $n = 100$, based on $N = 10000$ repetitions. For various adaptive BH procedures, we report the FDR and the power relative to the oracle procedure, which is the adaptive BH that uses the unknown true value of π_0 . In Figure 4, we consider fixed nonzero mean $\mu_1 = 3$ and changing true null proportion values on the x -axes. In Figure 5 we consider fixed $\pi_0 = 0.75$ and changing nonzero mean μ_1 on the x -axes.

The methods included in simulations defined in the main paper are ST-MED, ST-1/2, and LSL. DOS-1 and DOS-1/2 correspond to our proposed DOS-Storey procedures. ST-alpha corresponds to Storey's proportion estimator with $\lambda = \alpha$, the desired level of the FDR control, here set to 0.05. Simulations in Blanchard and Roquain (2009) show that ST-alpha works particularly well in the presence of dependence. Regarding independence, Blanchard and Roquain (2009) single out ST-1/2 as the best proportion estimator for adaptive FDR control. The approach proposed by Storey and Tibshirani (2003), as implemented in the function `pi0est` from the R package `qvalue`, requires a larger number of p -values near 1. This requirement makes the method unsuitable for situations involving smaller sample sizes or dependency.

In the top right plot of Figure 4, we see that under independence, and if the signal is sparse, the DOS methods have higher power than the ST-1/2 method. However, the FDR is slightly above $\alpha = 0.05$ in this small sample case. Under dependence, the DOS methods do not strictly control the FDR at the desired level $\alpha = 0.05$; the FDR is controlled at around 0.06. The power under dependence is comparable to that of ST- α , although with slightly weaker FDR control. Similar conclusions can be drawn from Figure 5. The DOS-1 method produces slightly more conservative estimates, which results in better FDR control. DOS methods behave stable when dependence is introduced and yield meaningful adaptive BH procedures under both independence and dependence.

We also include simulation results for larger sample sizes $n \in \{500, 1000, 5000\}$ under independence, based on $N = 1000$ repetitions. This sample size allows us to include the method by Storey and Tibshirani (2003) (STS), which is most commonly used in the applied literature. The FDR and relative power of various adaptive BH procedures are shown in Figure 6. It can be noted that the FDR control of the STS method is slightly above the desired level $\alpha = 0.05$, which is more prominent in small sample sizes. On the other hand, for large sample sizes, the DOS methods are more conservative and keep the FDR controlled below α .

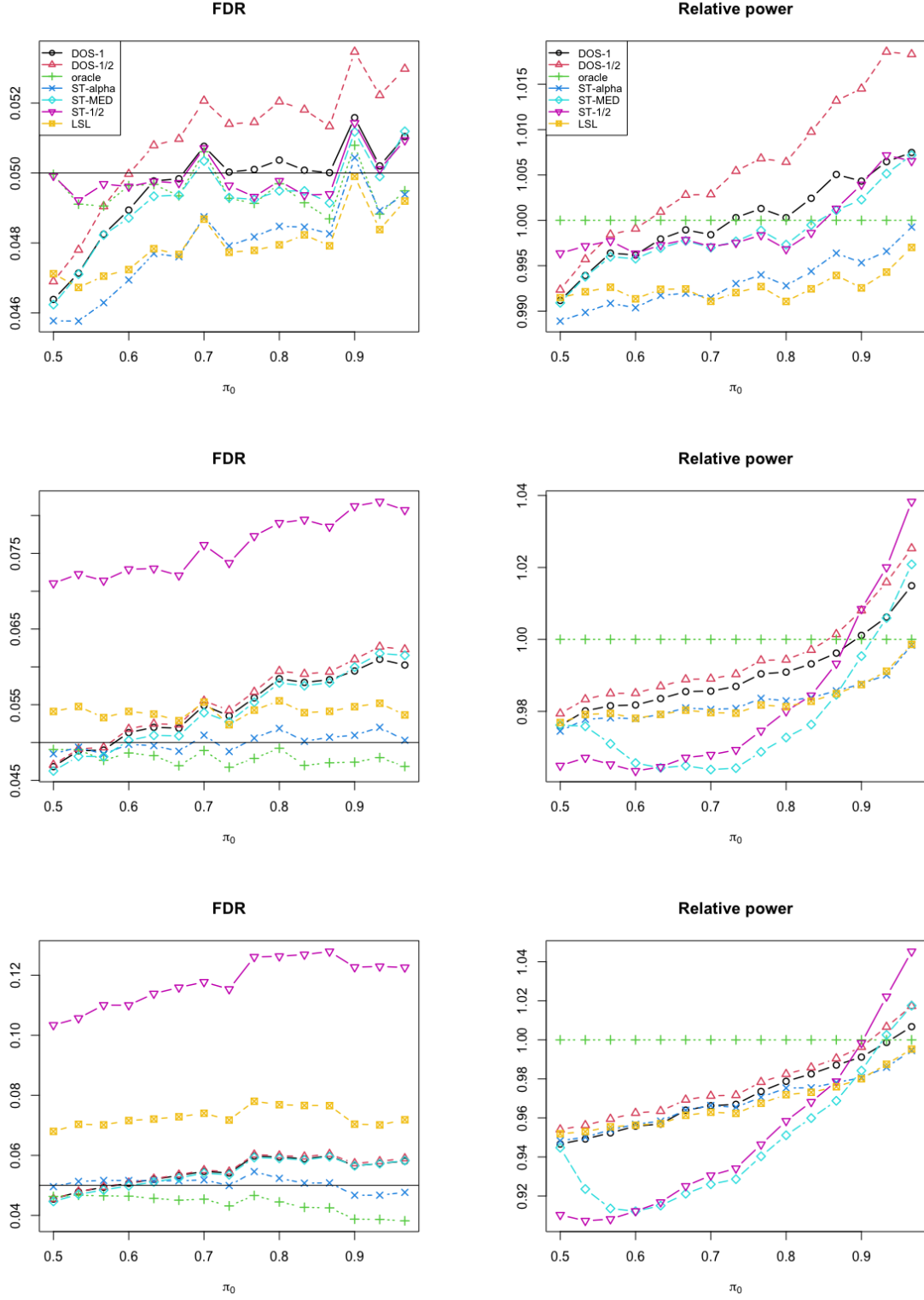


Figure 4: FDR and power relative to oracle as a function of the true null proportion π_0 , with $\mu_1 = 3$, for various adaptive BH procedures. From top to bottom: correlation coefficient $\rho \in \{0, 0.2, 0.5\}$.

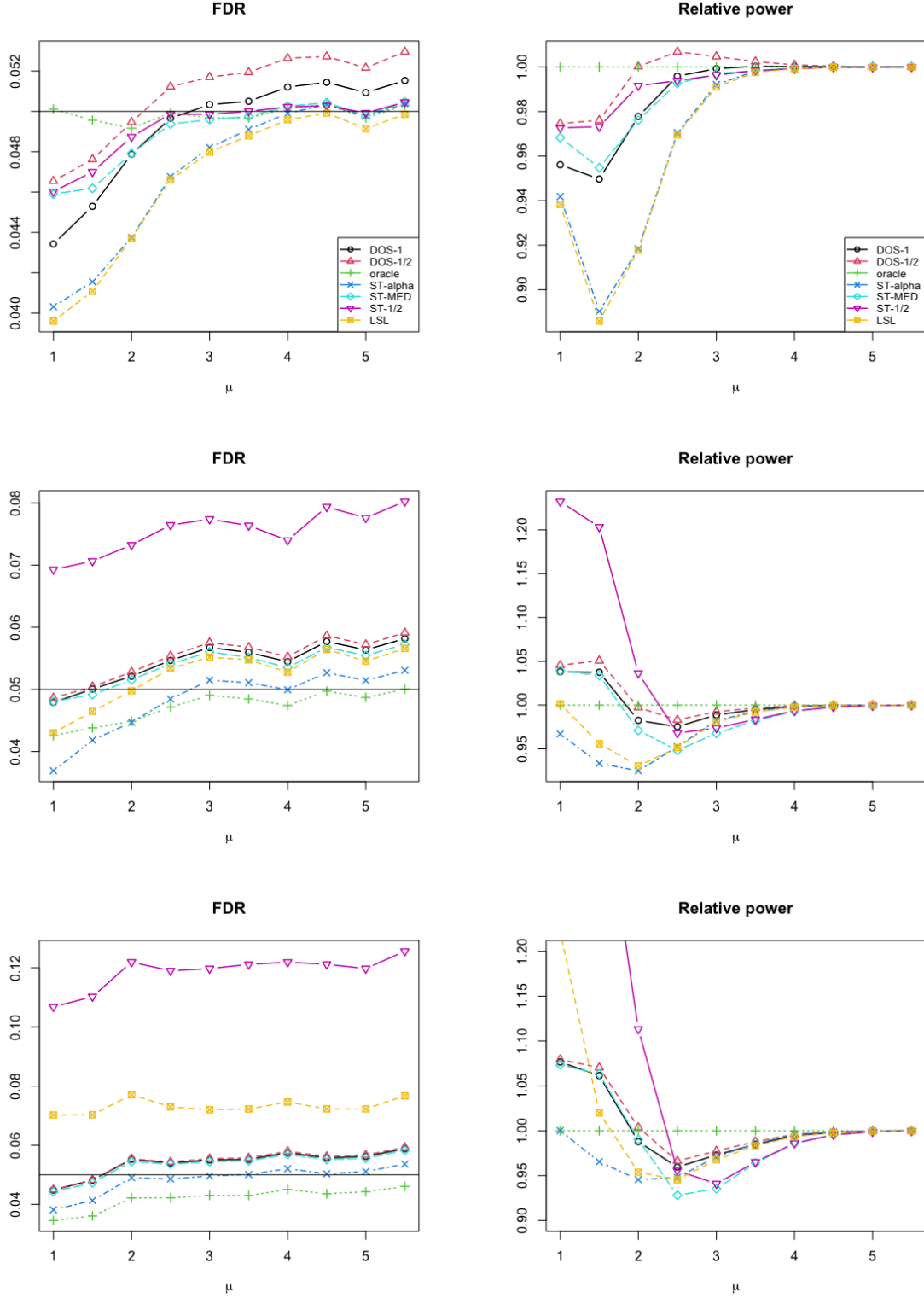


Figure 5: FDR and power relative to oracle as a function of the signal strength under the alternative, where $\pi_0 = 0.75$, for various adaptive BH procedures. From top to bottom: correlation coefficient $\rho \in \{0, 0.2, 0.5\}$.

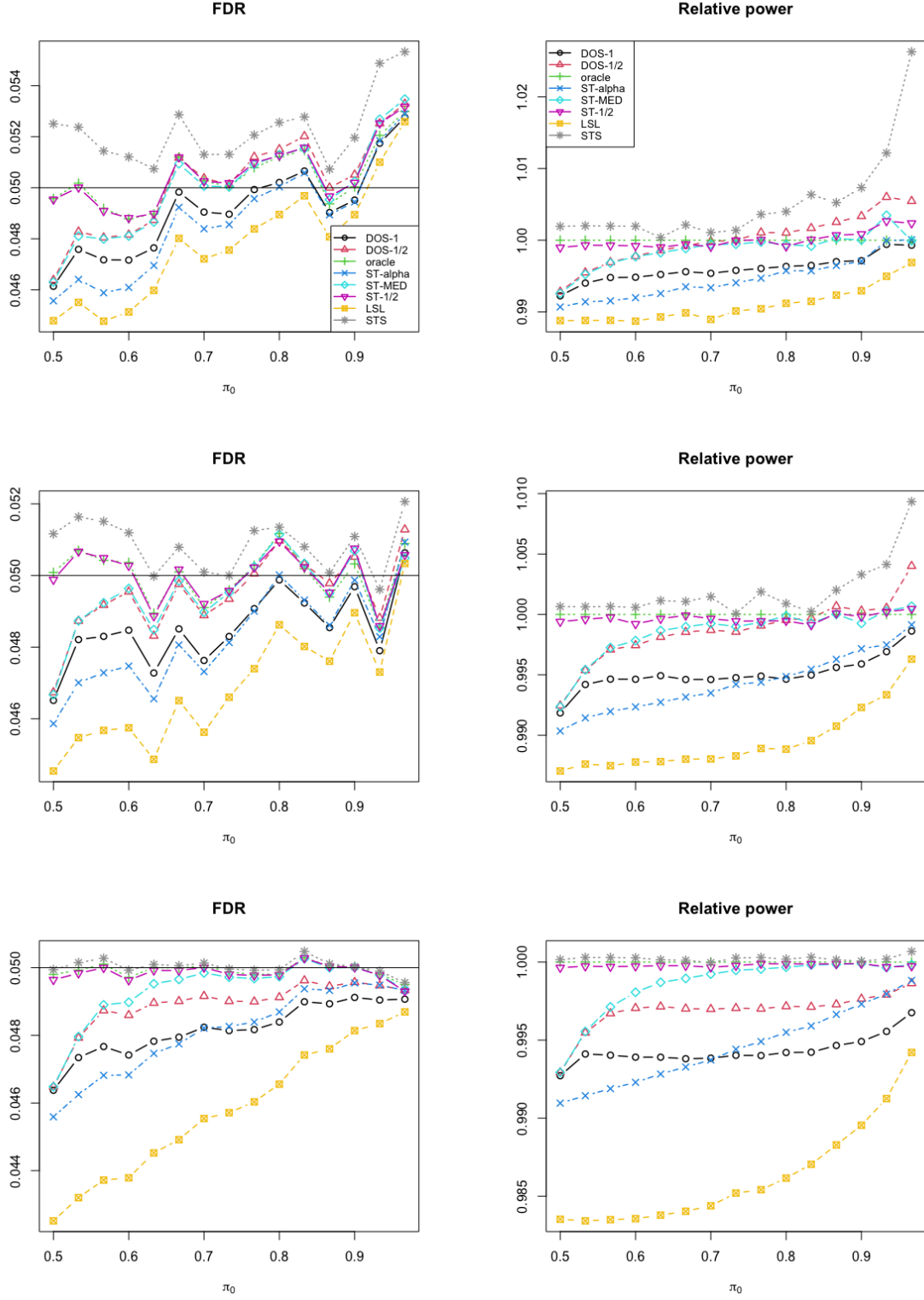


Figure 6: FDR and power relative to oracle as a function of the true null proportion π_0 , with $\mu_1 = 3$, for various adaptive BH procedures in case of large sample. From top to bottom: the size of the sample is $n \in \{500, 1000, 10000\}$.

B.3 Numerical Results for the Gaussian Mixture Model

In this section, we investigate the ideal asymptotic quantities from Theorem 1 to which the change-point location \hat{k}_α/n and the proportion estimator $\hat{\pi}_1^\alpha$ are converging to:

$$\hat{k}_\alpha/n \xrightarrow{a.s.} \operatorname{argmax}_{0 \leq t \leq 1/2} \frac{F^{-1}(2t) - 2F^{-1}(t)}{t^\alpha} \quad (3)$$

$$\hat{\pi}_1^\alpha \xrightarrow{a.s.} \frac{\tilde{t}_\alpha - F^{-1}(\tilde{t}_\alpha)}{1 - F^{-1}(\tilde{t}_\alpha)}. \quad (4)$$

We denote the asymptotic quantities on the right-hand side of equations (3) and (4) as \tilde{t}_α and $\tilde{\pi}_1^\alpha$ respectively. $\tilde{\pi}_1^\alpha$ is generally smaller than the true proportion, and we call this quantity the estimable proportion. To gain insights into the behavior of these asymptotic quantities, we perform computations of \tilde{t}_α and $\tilde{\pi}_1^\alpha$ under the Gaussian model. The numerical results are obtained using **Mathematica** and can be found within the **MTCP** package. The test statistics have a distribution that is a mixture of Gaussians:

$$T \sim \pi_1 N(\mu_1, 1) + \pi_0 N(0, 1) \quad (5)$$

where $\mu_1 > 0$. Denote

$$\Psi_{\mu_1}(t) = P(N(\mu_1, 1) \geq t) \quad (6)$$

$$\tilde{F}(t) = P(T \geq t) = \pi_1 \Psi_{\mu_1}(t) + (1 - \pi_1) \Psi_0(t). \quad (7)$$

One-sided p -values have the distribution with the CDF:

$$F(x) = P(p \leq x) = P(\Psi_0(T) \leq x) \quad (8)$$

$$= P(T \geq \Psi_0^{-1}(x)) \quad (9)$$

$$= \tilde{F}(\Psi_0^{-1}(x)) \quad (10)$$

$$= \pi_1 \Psi_{\mu_1}(\Psi_0^{-1}(x)) + (1 - \pi_1)x \quad (11)$$

Figure 7 shows $\tilde{\pi}_1^\alpha/\pi_1$ as a function of π_1 and for different values of the nonzero mean μ_1 . This quantity is shown for the two DOS-Storey estimators, for $\alpha = 1/2$ (left-hand plot) and $\alpha = 1$ (right-hand plot). $\tilde{\pi}_1^\alpha/\pi_1$ represents the ratio of the estimable proportion and the true proportion under this model. Similarly, Figure 8 shows \tilde{t}_1^α/π_1 as a function of π_1 and for different values of the nonzero mean μ_1 . For larger signal values, the change-point location gets close to the false null proportion.

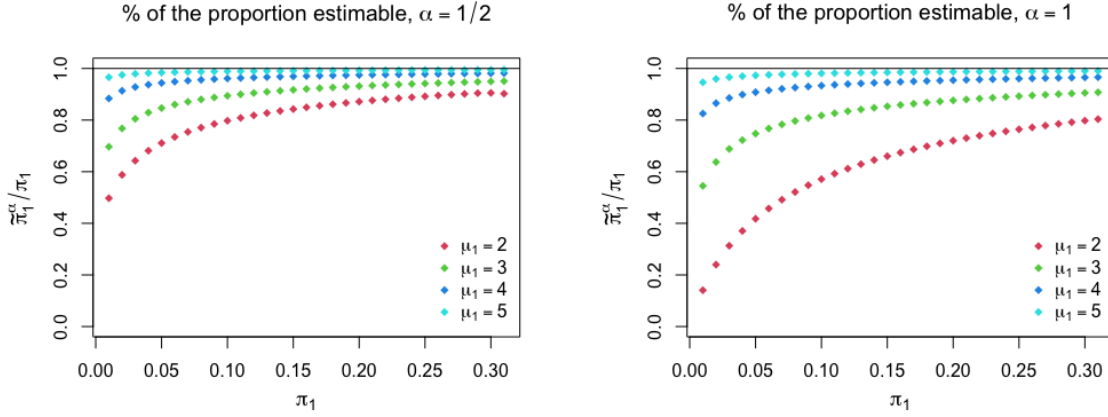


Figure 7: The percentage of the false null proportion the DOS method is able to estimate asymptotically in the Gaussian model, for $\alpha = 1/2$ (left) and $\alpha = 1$ (right) and various values of π_1 and μ_1 .

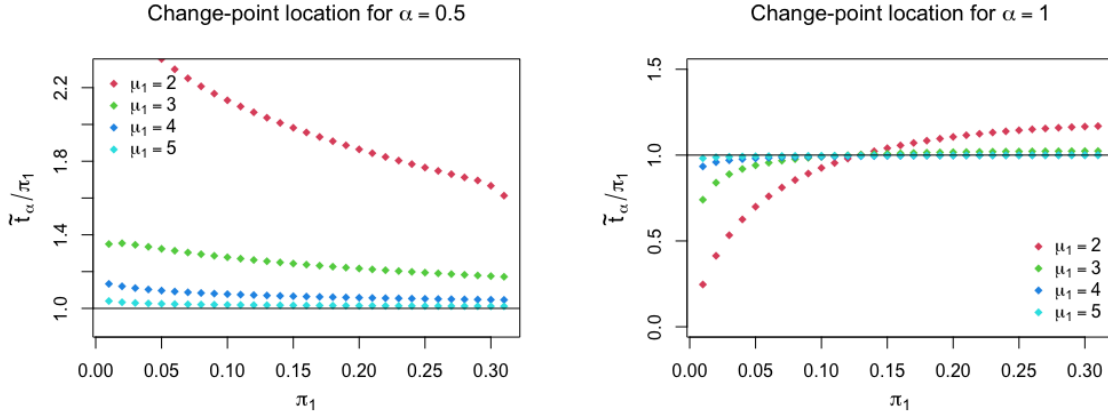


Figure 8: The percentage of the false null proportion the DOS method is able to estimate asymptotically in the Gaussian model, for $\alpha = 1/2$ (left) and $\alpha = 1$ (right) and various values of π_1 and μ_1 .

B.4 Dependence on c_n

In this section, we examine the impact of c_n on the DOS-Storey estimates under the Gaussian model. c_n is the proportion of values excluded from the DOS sequence when looking for a maximum (a change-point). We investigate how varying c_n influences the change-point and proportion estimates for different sample sizes $n \in 100, 1000, 10000, 100000$, as well as different values of the nonzero mean μ_1 and the false null proportion π_1 .

The results are presented in Figures 9.

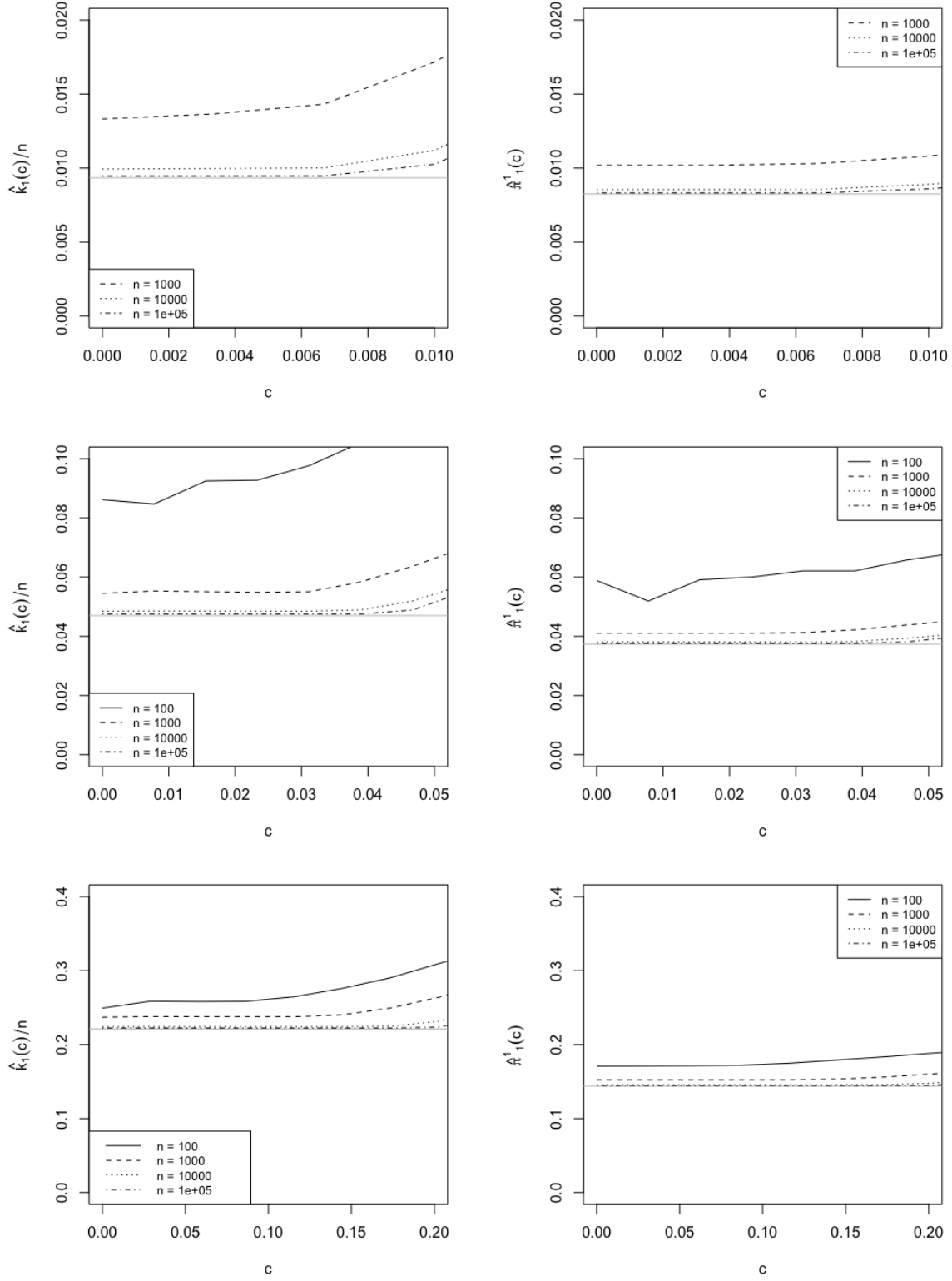


Figure 9: Averaged DOS change-point estimates (left column) and the DOS-Storey $\alpha = 1$ proportion estimates (right column) as a function of the proportion of excluded values (c) from the DOS sequence. The data is simulated from the Gaussian model. Top row: $\mu_1 = 4, \pi_1 = 0.01$, Middle row: $\mu_1 = 3, \pi_1 = 0.05$, Bottom row: $\mu_1 = 2, \pi_1 = 0.2$.

In the left-hand plots, we illustrate the mean estimated change-point location as a function of c , representing the proportion of excluded values. These estimates are averaged over $N = 1000$ repetitions, with each curve in the legend corresponding to a different sample size, n . The right-hand plots display the mean estimated proportion as a function of c , again averaged over $N = 1000$ repetitions, for various sample sizes, n . Furthermore, these plots effectively illustrate the convergence of the estimated change-point location and the estimated proportion towards the ideal values defined in Theorem 1 in the main paper, represented by the solid horizontal grey lines, as n increases.

Notably, in many of the scenarios we consider, the estimates remain stable. The estimates become sensitive when we exclude “too many” values which in general happens as c approaches π_1 . Additionally, sensitivity to the parameter c is more pronounced when the signal is weaker, as evidenced in Figure 10. Furthermore, these results reveal that the estimator performs well for small sample sizes. However, as the sample size grows, if the nonzero mean is not sufficiently large, the quantile function of the p -values becomes smoother, leading to increased variability in the change-point location.

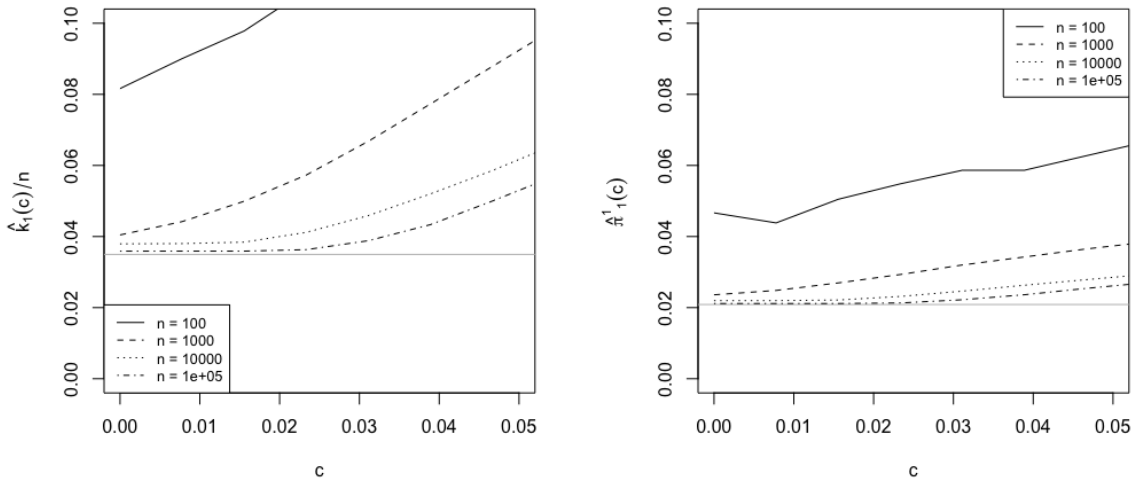


Figure 10: Averaged DOS change-point estimates (left column) and the DOS-Storey $\alpha = 1$ proportion estimates (right column) as a function of the proportion of excluded values (c) from the DOS sequence. The data is simulated from the Gaussian model with $\mu = 2$ and $\pi_1 = 0.05$. This plot shows that for weaker effects the estimates are more variable.

B.5 Comparing DOS to Other Change-Point Methods

In this section, we compare the performance of the DOS-Storey methods to the other change-point-based estimators in the literature. The simulation settings are as those in Table 1 from the main paper, and the change-point based methods included are by Hwang et al. (2014) (HKWL) and Turkheimer et al. (2001) (TSS). The results are shown in Table 3.

	DOS1	DOS05	HKWL	TSS
$\mu_1 = 3.5, \pi_1 = 0.01, n_1 = 10$				
BIAS	<u>-0.4</u>	9.9	-7.7	-0.4
SD	3.9	15.5	<u>1.5</u>	21.8
RMSE	<u>4.0</u>	18.4	7.8	21.8
$\mu_1 = 3.5, \pi_1 = 0.03, n_1 = 30$				
BIAS	-2.6	6.1	-18.9	<u>-1.6</u>
SD	5.4	12.9	<u>4.2</u>	19.6
RMSE	<u>6.0</u>	14.2	19.3	19.7
$\mu_1 = 3, \pi_1 = 0.1, n_1 = 50$				
BIAS	-8.8	4.8	-38.3	<u>-2.7</u>
SD	7.8	16.2	<u>5.7</u>	19.2
RMSE	<u>11.8</u>	16.9	38.7	19.4
$\mu_1 = 2, \pi_1 = 0.1, n_1 = 100$				
BIAS	-38.8	<u>-5.7</u>	-97.2	-27.1
SD	20.0	24.0	<u>2.6</u>	20.3
RMSE	43.7	<u>24.7</u>	97.3	33.9
$\mu_1 = 3, \pi_1 = 0.1, n_1 = 100$				
BIAS	-13.6	<u>1.6</u>	-53.8	-7.0
SD	10.4	16.7	<u>9.2</u>	19.1
RMSE	17.1	<u>16.8</u>	54.5	20.4
$\mu_1 = 2, \pi_1 = 0.2, n_1 = 200$				
BIAS	-47.1	<u>-15.5</u>	-179.2	-49.3
SD	26.5	23.5	<u>19.6</u>	20.3
RMSE	54.0	<u>28.1</u>	180.3	53.3
$\mu_1 = 3, \pi_1 = 0.2, n_1 = 200$				
BIAS	-20.2	<u>-3.3</u>	-58.2	-11.1
SD	12.7	16.5	<u>12.4</u>	18.5
RMSE	23.9	<u>16.8</u>	59.5	21.5
$\mu_1 = 3, \pi_1 = 0.3, n_1 = 300$				
BIAS	-23.5	<u>-5.8</u>	-52.6	-14.2
SD	14.1	15.5	<u>13.7</u>	17.5
RMSE	27.4	<u>16.6</u>	54.4	22.5

Table 3: Bias, standard deviation and the RMSE of the estimated number of the false null hypotheses ($n \times \hat{\pi}_1$), given the proportion of false null p -values π_1 , and the non-zero mean μ_1 , for a sample of size $n = 1000$, based on 200 repetitions. Bold and underlined values correspond to the smallest values in each row.

The HKWL method operates similarly to the DOS-Storey method. It involves fitting a piecewise linear function with one change-point to the sequence of p -values and then using the p -value at the identified change-point location as the parameter λ for Storey's estimator. However, this estimator tends to produce overly conservative estimates. The DOS-Storey estimates consistently outperform the HKWL estimates in nearly all cases. The TSS method, on the other hand, yields more precise estimates compared to the HKWL

method. Nonetheless, for small π_1 , both DOS-Storey with $\alpha = 1/2$ and $\alpha = 1$ have smaller Root Mean Square Error (RMSE) values. In cases with larger π_1 , DOS-Storey with $\alpha = 1/2$ consistently outperforms the TSS method.

C Interpretations

In this section we analyse how the DOS method relates to the methods available in the literature for estimating the knee/elbow point in a plot, by providing a short review of the papers on that topic. We proceed to give a short interpretation of the objective function h defined at the beginning of Section 3 of the main document.

C.1 Knee/Elbow Estimation

The methods used for estimating the knee/elbow in a plot are often heuristic, and the mathematical definition of this point is sometimes avoided. While some methods concentrate on estimating the point with the largest second derivative, the most natural approach to defining the knee/elbow is as the point where the curvature is maximized. The DOS method shares similarities with existing knee/elbow estimation methods - more precisely for elbow estimation, as the function of interest is convex. However, from this perspective, our objective function h_F^α presents a distinct definition for the elbow, better suited for the discrete nature of the data.

Detecting the knee/elbow in a graph is a problem of interest in model selection problems, such as estimating the number of factors in factor analysis or determining the optimal number of clusters. In their work, Salvador and Chan (2004) review several approaches and propose their method. Standard methods include finding the largest difference or the largest ratio between two consecutive points. The L-method proposed by Salvador and Chan (2004) consists of fitting two straight lines on each side of the candidate knee point and selecting the point with the smallest mean squared error as the estimated knee. In Antunes et al. (2018a) and Antunes et al. (2018b), the authors propose a thresholding-based method to identify the sharp angle in the plot, aiming to find the optimal transition point between the high and low values of the first derivative. Another widely used knee detection algorithm is proposed in Satopaa et al. (2011).

The DOS method can be seen as a method for estimating an elbow in a p -value plot. The DOS method can also be compared to the method for finding the sharpest angle in the graph of the quantile function. Simple analysis shows that the ideal change-point of the DOS method comes after the point where the sharpest angle is between points $(0, i/n)$ and $(i/n, 2i/n)$ on the graph. In that sense, the DOS method may be better seen as a method for estimating the point where the curvature drops significantly rather than the method for finding the point of the maximum curvature.

C.2 Scanning for the Largest Difference

We further analyse the objective function h defined at the beginning of Section 3 of the main document as:

$$h_F^\alpha(t) = \frac{F^{-1}(2t) - 2F^{-1}(t)}{t^\alpha}, \quad t \in (0, 1/2). \quad (12)$$

Define

$$H^\alpha(t, a) := \frac{F^{-1}(t+a) - F^{-1}(t)}{a^\alpha} - \frac{F^{-1}(t) - F^{-1}(t-a)}{a^\alpha}, \quad (13)$$

for $a \in (0, t]$ and $t \in [0, 1]$. For $a = t$, it holds that $H^\alpha(t, t) = h_F^\alpha(t)$.

Under the assumption of the existence and continuity of the first two derivatives of $(F^{-1})(t)$ on $t \in [0, 1]$, and considering that $(F^{-1})'$ is an increasing function, it follows that $H^\alpha(t, a)$ is increasing in a for any fixed t . Let $\tilde{t}_\alpha = \operatorname{argmax}_t h_F^\alpha(t)$. If $\tilde{t}_\alpha \leq 1/2$, it holds that

$$(\tilde{t}_\alpha, \tilde{t}_\alpha) = \operatorname{argmax}_{(t,a)} H^\alpha(t, a) = \operatorname{argmax}_{(t,t)} H^\alpha(t, t),$$

suggesting that the DOS statistic essentially estimates the point of the largest scaled difference on symmetric intervals of arbitrary length in the quantile function. We note that this interpretation is possible under the concavity assumption and assumption (A1). Scanning through all possible window sizes a is unnecessary and would introduce additional noise to the estimator, however, this perspective provides an interpretation that resembles the scan statistic commonly used in change-point analysis.

Lastly, we note that for small fixed values of a , the function $H(t, a)$ can be interpreted in terms of the second derivative $(F^{-1})''(t)$. By employing a second-order Taylor expansion, we obtain the following approximation:

$$H(t, a) = a(F^{-1})''(t) + o(a).$$

Thus, for small a and any $t \in (0, 1)$, maximising $H(t, a)$ is approximately equivalent to maximising the second derivative of F^{-1} . However, for larger a this approximation does not hold anymore, and the change point depends on the behaviour of the quantile function on the whole interval.

References

- Antunes, M., Gomes, D., and Aguiar, R. L. (2018a). Knee/elbow estimation based on first derivative threshold. In *2018 IEEE Fourth International Conference on Big Data Computing Service and Applications (BigDataService)*, pages 237–240.
- Antunes, M., Ribeiro, J., Gomes, D., and Aguiar, R. L. (2018b). Knee/elbow point estimation through thresholding. In *2018 IEEE 6th International Conference on Future Internet of Things and Cloud (FiCloud)*, pages 413–419.
- Benjamini, Y. and Hochberg, Y. (1995). Controlling the False Discovery Rate: A Practical and Powerful Approach to Multiple Testing. *Journal of the Royal Statistical Society: Series B*, 57, 289–300.

- Benjamini, Y. and Hochberg, Y. (2000). On the Adaptive Control of The False Discovery Rate in Multiple Testing With Independent Statistics. *Journal of Educational and Behavioral Statistics*, 25, 60–83.
- Blanchard, G. and Roquain, É. (2009). Adaptive False Discovery Rate Control Under Independence and Dependence. *Journal of Machine Learning Research*, 10, 2837–2871.
- Hoang, A.-T. and Dickhaus, T. (2020). On the Usage of Randomized p-Values in the Schweder–Spjøtvoll Estimator. *Annals of the Institute of Statistical Mathematics*, 74, 289–319.
- Hwang, Y. T., Kuo, H. C., Wang, C. C., and Lee, M. F. (2014). Estimating the Number of True Null Hypotheses in Multiple Hypothesis Testing. *Statistics and Computing*, 24, 399–416.
- Salvador, S. and Chan, P. (2004). Determining the number of clusters/segments in hierarchical clustering/segmentation algorithms. In *16th IEEE International Conference on Tools with Artificial Intelligence*, pages 576–584.
- Satopaa, V., Albrecht, J., Irwin, D., and Raghavan, B. (2011). Finding a "kneedle" in a haystack: Detecting knee points in system behavior. In *2011 31st International Conference on Distributed Computing Systems Workshops*, pages 166–171.
- Storey, J. D. and Tibshirani, R. (2003). Statistical Significance for Genomewide Studies. *Proceedings of the National Academy of Sciences*, 100, 9440–9445.
- Turkheimer, F. E., Smith, C. B., and Schmidt, K. (2001). Estimation of The Number of “True” Null Hypotheses in Multivariate Analysis of Neuroimaging Data. *NeuroImage*, 13, 920–930.